

N71-19912

(ACCESSION NUMBER)

(THRU)

(PAGES)

(CODE)

NASA CR-66762

(NASA CR OR TMX OR AD NUMBER)

(CATEGORY)

# TECHNICAL REPORT

## A SECOND-ORDER SLENDER-WING THEORY FOR WINGS WITH LEADING-EDGE SEPARATION

By: Joseph P. Nenni & Chee Tung

**CAL No. BB-2530-S-1**

**Prepared For:**

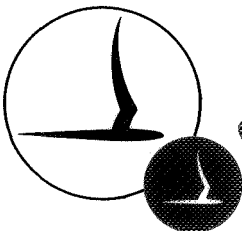
National Aeronautics and Space Administration  
Langley Research Center  
Langley Station  
Hampton, Virginia 23365

**FINAL REPORT**

NASA Contract NAS1-7650  
April 1969

**FOR NASA INTERNAL USE ONLY**

Distribution of this report is provided in the interest of  
information exchange. Responsibility for the contents  
resides in the author or organization that prepared it.



**CORNELL AERONAUTICAL LABORATORY, INC.**

OF CORNELL UNIVERSITY, BUFFALO, N. Y. 14221

## TABLE OF CONTENTS

	<u>Page</u>
SUMMARY	iii
LIST OF SYMBOLS	v
INTRODUCTION	1
MATCHED ASYMPTOTIC EXPANSION APPROACH	4
THE UNSEPARATED FLOW CASE	6
THE SEPARATED FLOW CASE	18
DISCUSSION OF RESULTS AND CONCLUSIONS	25
REFERENCES	26
APPENDIX A - DRASKY FLOW MODEL	28
APPENDIX B - BROWN AND MICHAEL FLOW MODEL	32
DISTRIBUTION LIST	42

## SUMMARY

A second-order, slender-wing theory has been developed for incompressible flow over low-aspect-ratio wings with and without leading-edge separation. The theory is second order in terms of the ratio of span to chord which is proportional to aspect ratio. The theory has been developed using the technique of matched asymptotic expansions. The Brown and Michael flow model was used for the case with leading-edge separation. The theory proves to be somewhat limited in that it can only be reasonably applied to wings which satisfy the Kutta condition at the trailing edge in the first approximation. The present results obtained for an aspect-ratio-one gothic wing represent a significant improvement for the separated flow case over the first-order result but the predicted lift is still somewhat higher than the experimental data.

## LIST OF SYMBOLS

$a$	ratio of half span to half root chord, $b/c$
$R$	aspect ratio
$b$	half span of wing at trailing edge
$c$	half root chord
$\bar{c}$	reference chord for pitching-moment coefficient
$C_L$	lift coefficient = $\frac{\text{Lift}}{\frac{1}{2} \rho U_\infty^2 S_{ref}}$
$C_{L\alpha}$	lift curve slope $\left( \frac{\partial C_L}{\partial \alpha} \right)_{\alpha=0}$
$C_m$	pitching-moment coefficient about $x_{m.c.}$ = $\frac{\text{Moment}}{\frac{1}{2} \rho U_\infty^2 S_{ref} \bar{c}}$
$C_{m\alpha}$	pitching-moment curve slope $\left( \frac{\partial C_m}{\partial \alpha} \right)_{\alpha=0}$
$G_1$	function of $\chi$ defined by Equation (38)
$G_2$	function of $\chi$ defined by Equation (56)
$G_3$	function of $\chi$ defined by Equation (58)
$h(\chi)$	normalized half span of wing as a function of $\chi$
$I.P.$	designates imaginary part of complex quantity
$\bar{P}(\chi)$	spanwise integrated loading as a function of $\chi$
$P(\chi, \bar{z})$	local wing loading
$R.P.$	designates real part of complex quantity
$S(\chi)$	half span of the wing as a function of $\chi$

$\bar{S}$	normalized wing area
$S_{ref}$	wing reference area for force and moment coefficients = $2ac^2\bar{S}$
$t$	time
$U_\infty$	free-stream velocity
$x, y, z$	outer variables, physical variables normalized by $c$
$x_{m.c.}$	chordwise location of pitching-moment reference center
$X, Y, Z$	inner variables
$Y_1, Z_1$	coordinates of vortex core in cross-flow plane
$\alpha$	angle of attack
$\Gamma$	vortex strength
$\gamma(x, z)$	bound vorticity distribution on wing
$\epsilon$	semiapex angle of delta wing; also, a small parameter
$\lambda, \tau$	normalized vortex coordinates in transformed cross-flow plane
$\xi$	complex outer variable ( $= z + iy$ )
$\rho$	free-stream density
$\sigma$	complex inner variable ( $= Z + iY$ )
$\sigma_1$	location of vortex core in cross-flow plane ( $= Z_1 + iY_1$ )
$\Phi_j^i$	velocity potential for $j^{th}$ inner solution
$\phi_j^o$	velocity potential for $j^{th}$ outer solution

## INTRODUCTION

The nonlinear aerodynamic characteristics of low-aspect-ratio wings with angle of attack has been the subject of extensive theoretical and experimental investigations over the past several years. The prime motivation of these investigations has been the application to the low-speed aerodynamic problems of high-speed aircraft and lifting reentry vehicles.

The first analytical attacks on the problem were made by Legendre (Reference 1), Brown and Michael (Reference 2), Mangler and Smith (Reference 3), and Smith (Reference 4). Numerous experimental investigations have been conducted with some of the more fundamental low-speed studies being made by Peckham (Reference 5), Bergesen and Porter (Reference 6), Lemaire (Reference 7), and Wentz and McMahon (Reference 8). Thus far, the theoretical analysis of the problem gives results which grossly overestimate the lift. A semiempirical method which gives an accurate estimate of the total lift has been developed by Polhamus in Reference 9. However, means to accurately estimate loading distributions are still needed.

It has been established that the nonlinear behavior with angle of attack can be attributed to the spiral sheets of vorticity that emanate from the leading edges and form over the upper surface. The general features of such flows are indicated in Figure 1. The previously mentioned analytical attacks on the problem have been made via slender-wing theory employing the concept of two-dimensional analysis in the cross-flow plane. (The cross flow is the flow in planes transverse to the body axis.) References 1 through 4 differ in the manner in which the spiral vortex sheet is approximated in the cross-flow plane. For a wing without spanwise camber, the cross-flow model consists of a flat plate which represents the trace of the mean camber surface of the wing plus some representation of the two spiral sheets that emanate from the plate edges (i. e., the wing leading edge). The flow in the cross-flow plane is determined using complex variable theory employing the complex velocity potential  $W$  defined such that  $W = \phi + i\psi$  where  $\phi$  is the velocity potential and  $\psi$  is the stream function.  $\phi$  and  $\psi$  are solutions to Laplace's equation and are determined using the constraints that:

1. There is no flow through the plate (wing).
2. The spiral vortex sheet is a stream surface and cannot sustain a force.
3. The pressure at the edges of the plate (wing leading edge) is finite. This is referred to as the leading-edge Kutta condition.

Legendre (Reference 1) represented the spiral sheets simply by two concentrated vortices above the upper surface of the wing. Brown and Michael (Reference 2) represented the sheets by two concentrated vortices plus

branch cuts in the complex potential that connect each vortex to its corresponding plate edge. Mangler and Smith (Reference 3) and Smith (Reference 4) represented each sheet by segmented arcs terminated by a branch cut and a concentrated vortex.

The agreement between these theories and experiment is shown in Figure 2. It can be seen that, while these theories qualitatively give the right variation with angle of attack, they grossly overestimate the lift.

Several reasons for this discrepancy have been suggested. Primary among these have been the following:

1. For a flat delta wing, the solutions obtained are conical and violate the Kutta condition at the trailing edge.
2. The approximations to the spiral vortex sheet have not been sufficiently accurate.
3. The flow visualizations of References 7 and 8 indicate there may be secondary separation on the upper surface of the wing and the significant associated vortices are not accounted for in the theories.

To examine the significance of the first of the above suggestions, it would be necessary to develop a method to calculate the truly three-dimensional flow field over low-aspect-ratio wings. A rigorous treatment of the low-aspect-ratio-wing problem would require a lifting-surface theory in which the wing can be represented by a sheet of distributed bound vorticity. The Kutta condition is applied at all swept edges of the planform and at the trailing edge. Trailing vorticity is allowed to form at all swept edges and the trailing edge. The trailing vorticity formed at swept leading edges streams back over the upper surface of the wing. Such a flow model is shown in Figure 1. This represents a wing with a nonplanar wake. The tangency condition must be applied on the wing surface. Furthermore, the trailing vorticity must lie on stream surfaces; that is, there is no flow through the trailing sheets and no pressure discontinuity across them. Conservation of vorticity can be applied at all edges where trailing vorticity forms to relate the trailing and bound vorticity. In this fashion, then, the tangency conditions and the Biot-Savart laws result in an integral equation which, in principle, determines the strength of the bound vorticity similar to ordinary lifting-surface problems. The problem is greatly complicated, however, since the location of the trailing vorticity over the wing is unknown a priori. In principle, an iterative technique could be applied to arrive at a solution. However, the complexity of the problem has, thus far, made this type of approach to the problem intractable.

Therefore, it appears that a promising approach to examining three-dimensional effects would be to devise a method to modify or correct the slender-wing or cross-flow analysis. Such a method has been developed using the technique of matched asymptotic expansions.

While the objective was to treat the problem of separated flow over low-aspect-ratio wings, the techniques were developed first for application to the unseparated flow case. This approach provided the foundations upon which the analysis of the separated flow problem was based. The development for the unseparated flow case is presented for the sake of clarity and completeness of this report, although it duplicates, to some extent, the analyses of Wang in Reference 10\*. However, Wang did not consider the separated flow problem.

The results for the unseparated flow case are compared with available first-order theories and experimental data. The comparison reveals certain significant limitations of the analysis, particularly with regard to application to delta wings, which apply to the separated flow problem as well.

The development of the techniques of matched asymptotic expansions for consideration of the separated flow case is presented. Brown and Michael's cross-flow representation of the separated flow (Reference 2) was used as the first-order model in the inner solution. This flow model was selected because it is compatible with the matched asymptotic expansion approach and, although relatively simple, yields numerical results that are not significantly different from the more complex representations of Mangler and Smith (References 3 and 4). Although the cross-flow model of Mangler and Smith appears to correspond more closely to experimentally observed flows, it proves to be impractical for use in the present scheme.

A promising new cross-flow model was also considered which was based on a configuration studied by Drasky (Reference 11). This model offered the possibility of replacing the branch cut in Brown and Michael's model with a more realistic spiral vortex sheet without having to resort to a numerical solution like Mangler and Smith. These features make it particularly appealing for use in the matched asymptotic expansions analysis. Unfortunately, it was found that the model, in its present form, cannot satisfy all of the essential physical constraints of the problem. It was not pursued further although it is believed that minor modifications to the present model could eliminate its limitations. This investigation is reported in Appendix A.

---

\*This reference came to the authors' attention during the preparation of this report and the analyses presented were developed independently.



## MATCHED ASYMPTOTIC EXPANSION APPROACH

The theory of matched asymptotic expansions was originally developed for viscous flow problems. The fundamental details and original development of the technique may be found in Reference 12. An additional reference where applications to some nonviscous flow problems are considered is Reference 13. A concise statement of the techniques is given in Reference 14. Briefly, the fundamental ideas involved may be described as follows. It is assumed that the velocity potential can be expanded in a series in some small parameter  $\epsilon$  (in the present application, this parameter is the ratio of wing span to wing chord) and, furthermore, that this solution can be divided into two parts: one part, valid for small  $\epsilon$  far from the wing, called the outer solution and the other part, valid for small  $\epsilon$  near the wing, called the inner solution. In general, the inner and outer solutions cannot be completely determined from the boundary conditions which apply to each solution. This incompleteness is resolved by requiring certain compatibility between the solutions referred to as matching conditions. Following the notation of Reference 13, we denote the outer solution by  $\phi^o$  and the inner solution by  $\bar{\phi}^i$ .  $\phi^o$  is determined as

$$\phi^o = \phi^o(x, y, z; \epsilon) \sim \phi_0^o + f_1(\epsilon)\phi_1^o + f_2(\epsilon)\phi_2^o + \cdots f_n(\epsilon)\phi_n^o + \cdots$$

where

$$\phi_i^o = \phi_i^o(x, y, z); \quad i = 0, 1, \dots, n, \dots$$

The first  $m$  terms of this expansion will be called the  $m$ -term outer expansion. Here,  $x, y, z$  are referred to as outer variables and are chosen such that the leading term is not a function of  $\epsilon$ . The  $f_n$  are referred to as gage functions and have the property that

$$\lim_{\epsilon \rightarrow 0} \frac{f_n}{f_{n-1}} = 0.$$

Similarly,  $\bar{\phi}^i$  is determined as

$$\bar{\phi}^i = \bar{\phi}^i(X, Y, Z; \epsilon) = \bar{\phi}_0^i + f_1(\epsilon)\bar{\phi}_1^i + f_2(\epsilon)\bar{\phi}_2^i + \cdots f_n(\epsilon)\bar{\phi}_n^i + \cdots$$

and the first  $m$  terms of this expansion are referred to as the  $m$ -term inner expansion.  $X, Y, Z$  are the inner variables chosen such that the leading term is not a function of  $\epsilon$  and again

$$\lim_{\epsilon \rightarrow 0} \frac{f_n}{f_{n-1}} = 0.$$

The inner and outer variables are related by a function of  $\epsilon$ . We call the expansion obtained by substituting inner variables in the  $m$ -term outer expansion, expanding for small  $\epsilon$  and retaining the first  $n$  terms as the  $n$ -term inner expansion of the  $m$ -term outer solution. We abbreviate this as " $n$  inner ( $m$  outer)". Similarly, we can form the  $m$ -term

outer expansion of the  $n$ -term inner solution by substituting outer variables in the  $n$ -term inner solution and expanding to  $m$  terms. This is abbreviated as " $m$  outer ( $n$  inner)". The matching that we require between inner and outer solutions can then be stated as:

$$m \text{ outer } (n \text{ inner}) = n \text{ inner } (m \text{ outer}).$$

This is the asymptotic matching principle as presented in Reference 13.

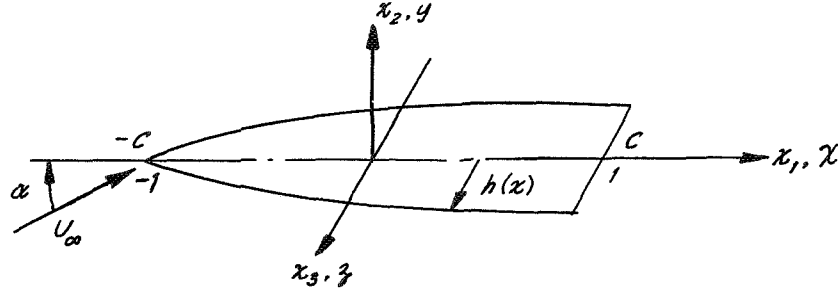
Van Dyke (Reference 15) has used this technique to develop a lifting-line-type theory for high-aspect-ratio wings. In the application of this technique to low-aspect-ratio wings, the cross-flow solution can be regarded as the first inner solution.

The slender-wing problem involves several small parameters in which an expansion could be considered such as thickness ratio, aspect ratio and angle of attack. The primary interest of this investigation is in the lifting problem for thin slender wings. Therefore, the interaction between thickness and angle-of-attack effects is neglected and the flow about an infinitely thin wing is considered. The matched asymptotic expansion approach is used to develop a theory which is of higher order in aspect ratio. The variation with angle of attack is determined by the cross-flow model which is used as the first inner solution. For example, in the unseparated flow problem, the cross-flow model consists of simply the flow normal to a flat plate with no free vorticity on the lee side. Hence, this inner solution results in a theory which is linear in angle of attack.

# THE UNSEPARATED FLOW CASE

## Coordinate System and Geometry

The flow about the wing is illustrated in the following sketch.



The dimensional variables are  $x_1, x_2, x_3$ .

The nondimensional variables are  $x = x_1/c$

$$y = x_2/c$$

$$z = x_3/c$$

where  $c$  is one-half the centerline chord. The equation of the wing leading edge is given by

$$z \pm b = ah(x)$$

where

$$a = b/c$$

and  $b$  is the half span of the wing. We require that  $h$  be a monotonically increasing function of  $x$  and  $a < 1$ .

We define a velocity potential  $\phi$  such that

$$u = \frac{\partial \phi}{\partial x} \frac{1}{c}; \quad v = \frac{\partial \phi}{\partial y} \frac{1}{c}; \quad w = \frac{\partial \phi}{\partial z} \frac{1}{c}$$

where  $u, v, w$  are the velocities in the  $x, y, z$  directions, respectively. The governing differential equation for  $\phi$  is Laplace's equation; i. e.,

$$\phi_{xx} + \phi_{yy} + \phi_{zz} = 0 \quad (1)$$

With boundary conditions appropriate for small angle of attack:

$$\text{Tangency } \phi_y = 0 \text{ for } y = 0, -1 \leq x \leq 1, |z| < a \cdot h \quad (2a)$$

$$\begin{aligned} \text{Upstream } \phi \sim U_\infty c(x + ay) \text{ for } x \rightarrow -\infty \\ \text{and } z, y \rightarrow \infty \end{aligned} \quad (2b)$$

$$\text{Kutta condition } \phi_x, \phi_y, \phi_z \text{ bounded at trailing edge of wing. (This condition will be discussed further.)} \quad (2c)$$

### Outer Limit Process

We can, as in conventional lifting-surface theory, represent the wing by a distribution of bound vorticity and the wake by trailing vorticity. The strength of the trailing vorticity is determined by the Helmholtz laws and the bound vorticity is determined by the tangency condition. Such a solution is

$$\phi = c U_{\infty}(x + \alpha y) + \frac{c}{4\pi\rho U_{\infty}} \int_{-1}^1 \int_{-ah}^{ah} y \frac{P(x_0, z_0)}{(z - z_0)^2 + y^2} \left[ 1 + \frac{(x - x_0)}{[(x - x_0)^2 + (z - z_0)^2 + y^2]^{\frac{1}{2}}} \right] dz_0 dx_0 \quad (3)$$

where  $P(x_0, z_0)$  is the local pressure loading which is related to the bound vorticity distribution by

$$\rho U_{\infty} \gamma(x_0, z_0) = P(x_0, z_0)$$

where  $\gamma(x_0, z_0)$  is the local bound vorticity distribution. The outer solution is then the limit of this solution as  $a$  becomes small with  $x, y, z$  fixed. Now, for small  $a$ , Equation (3) becomes

$$\phi \rightarrow \phi^o = c U_{\infty}(x + \alpha y) + \frac{c}{4\pi\rho U_{\infty}} y \int_{-1}^1 \frac{\bar{P}(x_0)}{z^2 + y^2} \left\{ 1 + \frac{(x - x_0)}{[(x - x_0)^2 + y^2 + z^2]^{\frac{1}{2}}} \right\} dx_0 \quad (4)$$

where  $\bar{P}(x_0) = \int_{-ah}^{ah} P(x_0, z_0) dz_0$  and is yet undetermined.

Equation (4) represents the potential for a distribution of singularities along the  $x$ -axis from 1 to -1 of strength  $\bar{P}(x_0)$  and it is tentatively assumed that

$$\bar{P}(x_0) = \sum_{n=1}^{\infty} \bar{P}_n(x_0) (a^2)^n.$$

Then, Equation (4) becomes

$$\phi^o = c U_{\infty}(x + \alpha y) + \frac{c}{4\pi\rho U_{\infty}} y \int_{-1}^1 \frac{\sum_{n=1}^{\infty} \bar{P}_n(a^2)^n}{z^2 + y^2} \left\{ 1 + \frac{(x - x_0)}{[(x - x_0)^2 + y^2 + z^2]^{\frac{1}{2}}} \right\} dx_0 \quad (5)$$

which is of the form  $\phi^o = \sum_{j=0}^{\infty} \phi_j^o a^{2j}$ .  $\bar{P}(x_0)$  will be determined by matching this outer solution with an inner solution.

### Inner Limit Process

To obtain the inner solution, we transform the problem using inner variables defined as

$$X = x ; Y = y/a ; Z = z/a$$

(i. e., we stretch the dimensions perpendicular to the line singularity or  $x$  axis). This transformation renders all relevant geometric quantities and derivatives with respect to  $X, Y, Z$  of order one in the vicinity of the  $X$ -axis. Since  $aX$  is a relevant transverse dimension as well as  $ah(X)$ ,

this then implies a restriction on  $\alpha$  such that  $\alpha/a$  is of order one. In terms of the boundary conditions, this is the same as saying that the disturbances transverse to the flow are all of the same order of magnitude.

We now seek a solution  $\Phi^i(X, Y, Z)$  valid in the vicinity of the  $X$  axis. Substitution of inner variables in Equation (1) leads to

$$a^2 \Phi_{XX}^i + \Phi_{YY}^i + \Phi_{ZZ}^i = 0 \quad (6)$$

with boundary conditions

$$\Phi_Y^i = 0 \quad \text{for} \quad Y = 0; \quad -1 \leq X \leq 1; \quad |Z| \leq h(X) \quad (7a)$$

$$\Phi^i \sim c U_\infty (X + a \alpha Y), \quad X \rightarrow -\infty \quad (7b)$$

$$\Phi_X^i, \Phi_Y^i, \Phi_Z^i \quad \text{bounded at trailing edge.} \quad (7c)$$

Equation (7c) will be discussed latter.

It is tentatively assumed that  $\Phi^i$  can be expanded as

$$\Phi^i = \sum_{j=0}^{\infty} \Phi_j^i a^j$$

The first gage function is determined by the upstream condition [Equation (7b)]. Substitution of this simple power series for  $\Phi^i$  in Equation (6) and the collection of terms of like powers of  $a$  yields

$$\Phi_{oYY}^i + \Phi_{oZZ}^i = 0 \quad (8)$$

$$\Phi_{iYY}^i + \Phi_{iZZ}^i = 0 \quad (9)$$

and for  $j \geq 2$

$$\Phi_{jYY}^i + \Phi_{jZZ}^i = -\Phi_{j-2XX}^i \quad (10)$$

Solution for  $\Phi_o^i$

$\Phi_o^i$  satisfies Equation (8) and  $\Phi_o^i \sim c X U_\infty$  for  $X \rightarrow \infty$ . We conclude that

$$\Phi_o^i = c U_\infty X \quad (11)$$

Solution for  $\Phi_i^i$

$\Phi_i^i$  satisfies Equation (9) and  $\Phi_i^i \sim c \alpha Y U_\infty$  for  $X \rightarrow \infty$ . Also,

$$\Phi_{iY}^i = 0 \quad -1 \leq X \leq 1, \quad |Z| \leq h(X).$$

We recognize these as the conditions for a flat plate of width  $h$  normal to a stream of velocity  $U_\infty a$  which has the solution

$$\bar{\Phi}' + i\bar{\Psi}' = -ic U_\infty a \sqrt{\sigma^2 - h^2} \quad (12)$$

where  $\sigma = Z + iY$ ,  $\bar{\Phi}$  and  $\bar{\Psi}$  are velocity potential and stream function, respectively. We are now in a position to determine  $\bar{P}_1(X)$  by matching.

### Matching

We now determine  $\bar{P}_1(X)$  by use of the "asymptotic matching principle" which has been stated in shorthand form as

$$m \text{ outer } (n \text{ inner}) = n \text{ inner } (m \text{ outer}).$$

We can accomplish this for  $n = m = 2$ . We start with the inner solution; the two-term inner solution is

$$\bar{\Phi}' = \bar{\Phi}'_0 + a\bar{\Phi}'_1 = cU_\infty X + a I.P. cU_\infty a \sqrt{\sigma^2 - h^2}. \quad (13a)$$

In view of the previous comments that  $(a/a)$  must be of order unity, Equation (13a) could have been equivalently expressed as

$$\bar{\Phi}' = cU_\infty X + a^2 I.P. cU_\infty (a/a) \sqrt{\sigma^2 - h^2}. \quad (13b)$$

This is the form of the well-established slender-body results of References 17, 18 and 19 which suggest that the first gage function should be  $a^2$  rather than  $a$  as in Equation (13a). It is also the form which we find is required in the investigation of the Drasky-type cross-flow model of separated flow discussed in Appendix A. However, in the present development, we shall continue to use Equation (13a).

Substitution of outer variables (i. e.,  $\xi = z + iy = a\sigma$ ) in Equation (13a) yields

$$\bar{\Phi}' = cU_\infty x + I.P. U_\infty a c \sqrt{\xi^2 - a^2 h^2}. \quad (14)$$

Expanded for small  $a$ ,

$$\bar{\Phi}' \sim cU_\infty x + I.P. U_\infty a c \left( \xi - \frac{1}{2} \frac{a^2 h^2}{\xi} - \frac{1}{16} \frac{a^4 h^4}{\xi^3} \right). \quad (15)$$

Now, retaining the first two terms in  $a$ , we have

$$\bar{\Phi}' \sim cU_\infty (x + ay) + \frac{a^2 h^2}{2} cU_\infty a \left( \frac{y}{y^2 + z^2} \right). \quad (16)$$

Back in terms of inner variables

$$\Phi^i \sim c U_\infty (X + a\alpha Y) + \frac{a h^2}{2} c U_\infty \alpha \left( \frac{Y}{Y^2 + Z^2} \right) \quad (17)$$

which is, in our abbreviated notation, "2 outer (2 inner)".

We now look at the outer solution. The two-term outer expansion is

$$\phi^o = c U_\infty (x + \alpha y) + \frac{c}{4\pi\rho U_\infty} y \int_{-1}^1 \frac{a^2 \bar{P}_1(x_o)}{y^2 + z^2} \left\{ 1 + \frac{(x - x_o)}{[(x - x_o)^2 + y^2 + z^2]^{\frac{1}{2}}} \right\} dx_o.$$

Expressed in terms of inner variables, this becomes

$$\begin{aligned} \phi^o &= c U_\infty (X + a\alpha Y) + \frac{acY}{4\pi\rho U_\infty} \int_{-1}^1 \frac{\bar{P}_1(X_o)}{Y^2 + Z^2} \left\{ 1 + \frac{(X - X_o)}{[(X - X_o)^2 + a^2(Y^2 + Z^2)]^{\frac{1}{2}}} \right\} dX_o. \\ &= c U_\infty (X + a\alpha Y) + \frac{acY}{4\pi\rho U_\infty} \frac{\partial^2}{\partial X^2} \int_{-1}^1 \frac{\bar{P}_1(X_o)}{Y^2 + Z^2} \left\{ \frac{(X - X_o)^2}{2} + \frac{(X - X_o)}{2} [(X - X_o)^2 \right. \\ &\quad \left. + a^2(Y^2 + Z^2)]^{\frac{1}{2}} + a^2 \frac{(Y^2 + Z^2)}{2} \sinh^{-1} \frac{(X - X_o)}{a\sqrt{Y^2 + Z^2}} \right\} dX_o \end{aligned} \quad (18)$$

Here we have integrated twice with respect to  $X$  under the integral sign and differentiated twice with respect to  $X$  outside the integral in order to avoid divergent terms in subsequent expansions. Expanded for small  $a$ , Equation (18) becomes

$$\begin{aligned} \phi^o &\sim c U_\infty (X + a\alpha Y) + \frac{acY}{4\pi\rho U_\infty} \frac{\partial^2}{\partial X^2} \int_{-1}^1 \frac{\bar{P}_1(X_o)}{Y^2 + Z^2} \frac{(X - X_o)}{2} [1 + \operatorname{sgn}(X - X_o)] dX_o \\ &\quad + \frac{a^3 c Y}{4\pi\rho U_\infty} \frac{\partial^2}{\partial X^2} \int_{-1}^1 \frac{\bar{P}_1(X_o)}{2} \operatorname{sgn}(X - X_o) \left\{ \frac{1}{2} + \ln \frac{2|X - X_o|}{a\sqrt{Y^2 + Z^2}} \right\} dX_o \end{aligned} \quad (19)$$

where, at this time, we need only retain the first two terms so that

$$2 \text{ inner (2 outer)} = c U_\infty (X + a\alpha Y) + \frac{acY}{4\pi\rho U_\infty} \int_{-1}^1 \frac{\bar{P}_1(X_o)}{Y^2 + Z^2} [1 + \operatorname{sgn}(X - X_o)] dX_o. \quad (20)$$

Matching the second terms of Equations (20) and (17), we obtain

$$\int_{-1}^1 \bar{P}_1(X_o) [1 + \operatorname{sgn}(X - X_o)] dX_o = h^2 2\pi\rho U_\infty^2 \alpha$$

or

$$2 \int_{-1}^X \bar{P}_1(X_o) dX_o = 2\pi\rho U_\infty^2 \alpha h^2. \quad (21)$$

Differentiating, obtain

$$\bar{P}_1(X) = 2\pi\rho U_\infty^2 \alpha h h'. \quad (22)$$

This result is equivalent to Jones' slender-wing result (Reference 16) and, for a delta wing, is readily integrated to yield

$$C_L = \pi\alpha \frac{AR}{2}.$$

To improve this result, we must obtain the third terms in the inner and outer solutions. Inspection of Equation (19) indicates that the next term in the inner solution should consist of an  $a^3$  term plus an  $a^3 \ln a$  term. Matching of the two outer (three inner) to the three inner (two outer) shows the nonexistence of any  $a^2$  term. Then,

$$\Phi^i \sim \Phi_0^i + a\Phi_1^i + a^3\Phi_{3,1}^i + a^3 \ln a \Phi_{3,2}^i \quad (23)$$

Inspection of Equation (15) shows that the next term in the outer expansion must be an  $a^4$  term but is not of the same type of singularity as  $\Phi_2^o$  [see Equation (5)]. However, we observe that

$$\frac{1}{\xi^3} = \frac{1}{2} \frac{d^2}{d\xi^2} \left( \frac{1}{\xi} \right) \text{ which suggests that}$$

$$\Phi_4^o = c \frac{\partial^2}{\partial z^2} y \int_{-1}^1 \frac{K(x_0)}{z^2 + y^2} \left\{ 1 + \frac{(x-x_0)}{[(x-x_0)^2 + y^2 + z^2]^{\frac{1}{2}}} \right\} dx_0 \quad (24)$$

where

$$\Phi^o \sim \Phi_0^o + a^2\Phi_2^o + a^4\Phi_4^o$$

and to determine  $K(x_0)$  we must match two inner (three outer) to three outer (two inner). Equation (15) is essentially the second expansion. We therefore proceed to calculate the first expansion.

We performed the differentiation with respect to  $z$  indicated in Equation (24). Then we integrated and differentiated twice with respect to  $x$  as in Equation (18) in order to avoid subsequent singular terms. Equation (24) then becomes

$$\begin{aligned} a^4\Phi_4^o = a^4 y c \frac{\partial^2}{\partial x^2} \int_{-1}^1 K(x_0) \left\{ \frac{(6z^2 - 2y^2)}{(z^2 + y^2)} \left[ \frac{(x-x_0)^2}{2} + \frac{(x-x_0)}{2} [(x+x_0)^2 + y^2 + z^2]^{\frac{1}{2}} \right] \right. \\ \left. - \frac{z^2}{y^2 + z^2} (x-x_0) [(x-x_0)^2 + y^2 + z^2]^{-\frac{1}{2}} \right\} dx_0 \end{aligned} \quad (25)$$



Substitution of inner variables, expansion for small  $\alpha$ , and performance of the differentiation yields

$$\begin{aligned}
a^4 \phi_4^0 &\sim aYc \int_{-1}^1 K(X_o) \frac{(6Z^2 - 2Y^2)}{(Z^2 + Y^2)^3} (1 + \text{sgn}(X - X_o)) dX_o \\
&\quad - a^3 Yc \frac{dK}{dX} \frac{(Z^2 - Y^2)}{(Z^2 + Y^2)^2}
\end{aligned} \tag{26}$$

where the second term is not presently needed but will be required for later matchings. We now can construct

$$\begin{aligned}
2 \text{ inner } (3 \text{ outer}) &= cU_\infty(X + a\alpha Y) + ac \frac{U_\infty}{2} \frac{Y\alpha}{Y^2 + Z^2} \int_{-1}^1 hh'(X_o)(1 + \text{sgn}(X - X_o)) dX_o \\
&\quad + acY \frac{(6Z^2 - 2Y^2)\alpha}{(Z^2 + Y^2)^3} \int_{-1}^1 K(X_o)(1 + \text{sgn}(X - X_o)) dX_o
\end{aligned} \tag{27}$$

where the first two terms have been matched previously [by matching Equations (17) and (20)]. Reexpressing Equation (15) in inner variables,

$$\begin{aligned}
3 \text{ outer } (2 \text{ inner}) &= cU_\infty(X + a\alpha Y) + \frac{a h^2}{2} cU_\infty \alpha \left( \frac{Y}{Y^2 + Z^2} \right) \\
&\quad + a \frac{U_\infty \alpha h^4}{16} cY \left( \frac{6Z^2 - 2Y^2}{(Z^2 + Y^2)^3} \right).
\end{aligned} \tag{28}$$

Matching the last term in Equation (27) with the last term in Equation (28), we conclude that

$$\int_{-1}^1 K(X_o) (1 + \text{sgn}(X - X_o)) dX_o = \frac{U_\infty \alpha h^4}{16}$$

or

$$K(X) = \frac{U_\infty \alpha h^3 h'}{8} \tag{29}$$

We now have the three-term outer expansion as

$$\begin{aligned}\phi^o = & c U_\infty (x + \alpha y) + a^2 \frac{c U_\infty \alpha}{2} y \int_{-1}^1 \frac{h h'(\chi_o)}{y^2 + z^2} \left\{ 1 + \frac{(x - x_o)}{[(x - x_o)^2 + y^2 + z^2]^{\frac{1}{2}}} \right\} d\chi_o \\ & + a^4 \frac{U_\infty \alpha c}{8} y \frac{\partial^2}{\partial z^2} \int_{-1}^1 \frac{h^3 h'}{y^2 + z^2} \left\{ 1 + \frac{(x - x_o)}{[(x - x_o)^2 + y^2 + z^2]^{\frac{1}{2}}} \right\} d\chi_o. \quad (30)\end{aligned}$$

The three-term inner expansion of this result is

$$\begin{aligned}3 \text{ inner } (3 \text{ outer}) = & c U_\infty (X + a \alpha Y) + a c \left\{ \frac{U_\infty \alpha}{2} h^2(X) \frac{Y}{Y^2 + Z^2} \right. \\ & + \frac{U_\infty \alpha h^4(X)}{16} Y \frac{(6Z^2 - 2Y^2)}{(Z^2 + Y^2)^3} \left. \right\} + a^3 c \left\{ \frac{U_\infty \alpha}{8} (h^3 h') Y \frac{(Z^2 - Y^2)}{(Z^2 + Y^2)^2} + \frac{U_\infty \alpha Y}{2} \left( \frac{(h h')'}{2} \right. \right. \\ & \left. \left. - (h h')' \ln \frac{\sqrt{Y^2 + Z^2}}{2} + \frac{1}{2} \frac{\partial^2}{\partial X^2} \int_{-1}^1 h h' \operatorname{sgn}(X - X_o) \ln |X - X_o| dX_o \right) \right\} - a^3 \ln a \left\{ (h h')' \frac{U_\infty \alpha Y}{2} \right\}. \quad (31)\end{aligned}$$

We now seek  $\Phi_{31}^i$  and  $\Phi_{32}^i$  such that the 3 outer (3 inner) is equal to Equation (31).

From Equation (10), we see that  $\Phi_{31}^i$  satisfies

$$\Phi_{31}^i{}_{YY} + \Phi_{31}^i{}_{ZZ} = -\Phi_{31}^i{}_{XX} = -\frac{\partial^2}{\partial X^2} I.P. c U_\infty \alpha \sqrt{\sigma^2 - h^2} \quad (32)$$

Then,  $\Phi_{31}^i$  must be composed of a complementary and particular solution; i. e.,

$$\Phi_{31}^i = \Phi_{31}^i(P) + \Phi_{31}^i(c)$$

The particular solution is most easily found by using the complex potential  $W_{31}^{(P)}$  where  $W_{31}^{(P)} = \Phi_{31}^i(P) + i\Psi_{31}^i(P)$ . This plus the substitution  $\sigma = Z + iY$  transforms Equation (32) to

$$4 \frac{\partial^2 W_{31}^{(P)}}{\partial \sigma \partial \bar{\sigma}} = \frac{\partial^2}{\partial X^2} \left\{ i U_\infty \alpha \sqrt{\sigma^2 - h^2} \right\} \quad (33)$$

which is readily integrated to

$$W_{31}^{(P)} = i \sigma \frac{U_\infty \alpha}{4} \left\{ \sigma h'^2 (\sigma^2 - h^2)^{-\frac{1}{2}} - (h h') \cosh^{-1} \frac{\sigma}{h} \right\} \quad (34)$$

and leads to

$$\Phi_{31}^i(P) = -I.P. \frac{\bar{\sigma} U_{\infty} \alpha c}{4} \left\{ \sigma h'^2 (\sigma^2 - h^2)^{-\frac{1}{2}} - (hh')' \cosh^{-1} \frac{\sigma}{h} \right\}.$$

We now choose  $\Phi_{31}^i(c)$  such that

- it satisfies  $\Phi_{31zz}^i(c) + \Phi_{31YY}^i(c) = 0$
- the outer limit of  $\Phi_{31}^i$  combines with  $\Phi_1^i$  to produce the  $a^3$  term of Equation (31), and
- there is no resultant flow through the surface.

Such a solution is found by inspection to be

$$\begin{aligned} \Phi_{31}^i(c) = I.P. & \left[ \frac{U_{\infty} \alpha h'^2}{4} \sigma^2 (\sigma^2 - h^2)^{-\frac{1}{2}} - (hh')' \sigma \frac{U_{\infty} \alpha}{4} \cosh^{-1} \frac{\sigma}{h} \right. \\ & \left. + \frac{U_{\infty} \alpha}{2} \sqrt{\sigma^2 - h^2} \left\{ (hh')' \left( \ln \frac{4}{h} + \frac{1}{2} \right) - h'^2 + \frac{\partial^2}{\partial X^2} \int_{-1}^1 \frac{hh'}{2} \operatorname{sgn}(X-X_0) \ln |X-X_0| dX_0 \right\} \right] \end{aligned} \quad (35)$$

$\Phi_{32}^i$  is found more easily. It satisfies the homogeneous equation

$$\Phi_{32YY}^i + \Phi_{32ZZ}^i = 0$$

and the tangency condition. It is found by inspection to be

$$\Phi_{32}^i = I.P. U_{\infty} \alpha c \sqrt{\sigma^2 - h^2} \frac{(hh')'}{2}. \quad (36)$$

We now can construct the three-term inner expansion

$$\Phi^i = \Phi_0^i + a \Phi_1^i + a^3 \Phi_{31}^i + a^3 \ln a \Phi_{32}^i$$

or

$$\begin{aligned} \Phi^i = & U_{\infty} c X + a I.P. U_{\infty} \alpha c \sqrt{\sigma^2 - h^2} \\ & + a^3 \frac{U_{\infty} \alpha c}{4} I.P. \left\{ (hh')' (\bar{\sigma} - \sigma) \cosh^{-1} \frac{\sigma}{h} + h'^2 \sigma (\sigma - \bar{\sigma}) (\sigma^2 - h^2)^{-\frac{1}{2}} \right. \\ & \left. + 2 \sqrt{\sigma^2 - h^2} G_1(X) \right\} - a^3 \ln a I.P. \left\{ \frac{c U_{\infty} \alpha}{2} (hh')' \sqrt{\sigma^2 - h^2} \right\} \end{aligned} \quad (37)$$

where

$$G_1(X) = (hh')' \left( \ln \frac{4}{h} + \frac{1}{2} \right) - h'^2 + \frac{\partial^2}{\partial X^2} \int_{-1}^1 \frac{hh'}{2} \operatorname{sgn}(X-X_0) \ln |X-X_0| dX_0. \quad (38)$$

We now have obtained the three-term inner and outer expansions.

## Results

It can be shown that the terms in  $\Phi'$  that involve  $(\sigma - \bar{\sigma})$  do not contribute to the lift. Therefore, we may use Blasius' theorem to determine the lift as

$$C_L = \frac{\pi \alpha}{2\bar{S}} \left( 2a + a^3 G_r(1) - a^3 \ln a \frac{1}{2} (h''(1) + h'_{\bar{r}}(1)) \right) \quad (39a)$$

where

$$\bar{S} = \int_{-1}^1 h(x) dx.$$

The pitching-moment coefficient is readily obtained as

$$\begin{aligned} C_m = & -\frac{c}{\bar{c}} (1 - x_{m.c.}) C_L + \frac{\pi \alpha}{2\bar{S}} \frac{c}{\bar{c}} \int_{-1}^1 \left\{ 2ah^2 \right. \\ & \left. + a^3 \left[ G_r(x)h^2 - \ln a (hh')' \frac{h^2}{2} \right] \right\} dx \end{aligned} \quad (39b)$$

where  $x_{m.c.}$  is the chordwise location of the moment reference center and  $\bar{c}$  is the reference chord.

The integral expression appearing in  $G_r(x)$  can be evaluated using the following formula derived from Reference 17:

$$\begin{aligned} \frac{\partial}{\partial x} \int_{-1}^1 F(x_0) \operatorname{sgn}(x - x_0) \ln|x - x_0| dx_0 &= F(x) \ln(1 - x^2) \\ &- \int_{-1}^1 \frac{F(x) - F(x_0)}{|x - x_0|} dx_0 \end{aligned} \quad (40)$$

This expression then can be differentiated once more to obtain the desired form; that is,

$$\begin{aligned} \frac{\partial^2}{\partial x^2} \int_{-1}^1 F(x_0) \operatorname{sgn}(x - x_0) \ln|x - x_0| dx &= \frac{\partial}{\partial x} \left\{ F(x) \ln(1 - x^2) \right. \\ &\left. - \int_{-1}^1 \frac{F(x) - F(x_0)}{|x - x_0|} dx_0 \right\} \end{aligned} \quad (41)$$

In general, for this integral to exist in the strict mathematical sense, the following must be true:

$$F(1) = F(-1) = 0 \quad (42a)$$

$$F'(1) = 0 \quad (42b)$$

$F$  is proportional to  $\bar{P}$  (the chordwise loading). If the wing apex is pointed, the condition that  $\bar{P}(-1) = 0$  is satisfied. The condition that  $\bar{P}(1) = 0$  is equivalent to the Kutta condition at the trailing edge. Equation (42b) imposes the additional restriction that the derivative of the chordwise loading at the trailing edge should also be zero. This leads to the following restrictions on planform:

$$h'(1) = 0 \quad (\text{Kutta condition}) \quad (43a)$$

$$h''(1) = 0 \quad (43b)$$

These restrictions were also encountered by Adams and Sears (Reference 20) in their not-so-slender wing theory.

If the concept of the "finite part of a divergent integral" (References 21 and 22) is used, the integral appearing in  $G_1(x)$  in Equation (38) can be evaluated for all planforms. This concept has been used to evaluate the lift curve slope as a function of  $x$  for two planforms. For a gothic-type wing with  $h = \frac{1}{4}(3+2x-x^2)$ , we obtain

$$C_{L\alpha} = \frac{3}{8}\pi \left( 2a - 0.318a^3 + \frac{a^3}{4} \ln a \right) \quad (44a)$$

$$C_{m\alpha} = -\frac{3}{4}C_{L\alpha} + \frac{\pi}{4} \left( 2.133a - 0.280a^3 + 0.152a^3 \ln a \right) \quad (44b)$$

where  $x_{m.c.} = -0.125$  and  $\frac{\bar{c}}{c} = 0.667$  to correspond with the experimental data of Reference 5. For delta wings,  $h = \frac{1}{2}(1+x)$  and

$$C_{L\alpha} = \frac{\pi}{2} \left( 2a - 0.02786a^3 - \frac{a^3}{8} \ln a \right) \quad (45)$$

These results are plotted in Figures 3, 4 and 5 where they are compared with first-order theory and limited experimental data. The results for the gothic wing appear quite reasonable. The results for a delta wing as represented by Equation (45) offers no significant improvement over Jones' theory. The gothic wing satisfies Equation (43a) but not Equation (43b). The delta wing satisfies Equation (43b) but not Equation (43a). This comparison suggests that useful results may be obtained provided the planform satisfies Equation (43a).

The problem encountered at the trailing edge in this theory is analogous to the one encountered by Van Dyke (Reference 15) at the wing tips of a high-aspect-ratio wing. We can expect problems in developing higher-order solutions when the first-order solution contains a jump discontinuity in the pressure when passing from the wing to the wake. Van Dyke (Reference 15) was able to circumvent this problem by devising another expansion valid in the immediate vicinity of the wing tips and then matching this solution with the solution valid over the remainder of the wing. This technique does not appear to be promising for our present

problem. Such a procedure, in this case, would transform the problem of the actual flow over the trailing edge to the problem of determining the flow over the trailing edge of a finite span wing with semi-infinite chord for which no solution is known at this time.

It does appear, however, that the problem can be solved by adding an additional distribution of singularities on the wing surface to the first-order solutions. These singularities should be such that the total solution meets the Kutta condition at the trailing edge. The first two terms in the inner solution would then be represented by

$$\Phi^i = U_\infty c x + a \text{ R.P. i.c. } \left\{ -U_\infty \alpha \sqrt{\sigma^2 - h^2} + f_1(x) F_1(\sigma; x) \right\}$$

where  $F_1(\sigma; x)$  is the additional distribution of singularities.  $F_1(\sigma; x)$  must be chosen to have certain asymptotic properties such that matching with an outer solution is possible.  $\partial F_1 / \partial x$  evaluated on the wing surface must contain a  $1/\sqrt{Z^2 - h^2}$  term to satisfy the Kutta condition all along the trailing edge, and  $F_1(\sigma; x)$  must preserve the tangency condition on the wing surface. Unfortunately, these constraints plus the boundary conditions expressed by Equations (2a) through (2c) do not determine  $f_1(x) F_1(\sigma; x)$  uniquely. A solution locally valid in the vicinity of the trailing edge must be developed to resolve this nonuniqueness.

## THE SEPARATED FLOW CASE

The development of the solution for the separated flow case follows lines similar to the unseparated case. The boundary conditions for the separated flow case are given by Equations (2a) through (2c) with the additional requirement of a Kutta condition at the leading edge as well as the trailing edge. The differences in the solution are introduced by the addition to the cross-flow model of a representation of the spiral vortex sheets that form on the lee side of the wing. The Brown and Michael cross-flow model has been used for this analysis.

A line distribution of doublets again proves adequate for the first outer solution (with the strength variation modified to account for the vortex formation). However, the vortex formation has a pronounced effect on the higher-order terms in the outer solution. As will be shown, the second term in the outer solution is now of order  $\alpha^3$  instead of  $\alpha^4$  as in the unseparated flow case.

In the inner solution, the order of the first two solutions is unaffected by the vortex formation although the solutions are considerably more complicated.

### Inner Solution

For the separated flow case, the cross-flow model of Brown and Michael (Reference 2) was used in formulating the first inner solution. In this model, the representation of the vorticity on the lee side of the plate consists of two concentrated vortices connected to their respective plate edges by branch cuts in the velocity potential. The details of this flow model and the method used to determine the vortex strength and location are discussed in Appendix B. For present purposes, we may consider the vortex strength and position as known functions of  $X$ .

The appropriate two-term inner solution for the Brown and Michael flow model is

$$\begin{aligned} \Phi^i = U_\infty \alpha c X - a.R.P. i \left\{ U_\infty \alpha c \sqrt{\sigma^2 - h^2} \right. \\ \left. + \frac{\Gamma_c}{2\pi} \ln \left( \frac{\sqrt{\sigma^2 - h^2} - \sqrt{\sigma_i^2 - h^2}}{\sqrt{\sigma^2 - h^2} + \sqrt{\sigma_i^2 - h^2}} \right) \right\} \end{aligned} \quad (46)$$

The vortices on the lee side of the wing are located at  $\sigma_i$  and  $-\sigma_i$ . The strength of each is  $\Gamma$ .

The outer expansions of Equation (46) required for matching and written in terms of inner variables are

$$\begin{aligned} 2 \text{ outer (2 inner)} &= U_{\infty} \alpha c X + a \left\{ U_{\infty} \alpha c Y \right. \\ &\quad \left. + \left( \frac{\Gamma c \lambda h}{\pi} + \frac{1}{2} h^2 U_{\infty} \alpha c \right) \frac{Y}{Y^2 + Z^2} \right\} \end{aligned} \quad (47a)$$

$$\begin{aligned} 3 \text{ outer (2 inner)} &= U_{\infty} \alpha c X + a \left\{ U_{\infty} \alpha c Y \right. \\ &\quad \left. + \left( \frac{\Gamma c \lambda h}{\pi} + \frac{1}{2} h^2 U_{\infty} \alpha c \right) \frac{Y}{Y^2 + Z^2} - \frac{\Gamma c Y_1 Z_1}{\pi} \frac{(Z^2 - Y^2)}{(Y^2 + Z^2)^2} \right\} \end{aligned} \quad (47b)$$

where the following substitutions have been used

$$\begin{aligned} \sqrt{\sigma_1^2 - h} &= (\lambda + i\tau) h \\ \sigma_1 &= Z_1 + i Y_1 \end{aligned}$$

### Outer Solution

The three-term outer solution is now

$$\begin{aligned} \phi^o &= U_{\infty} c (x + \alpha y) + a^2 \frac{y c}{4\pi \rho U_{\infty}} \int_{-1}^1 \frac{\bar{P}(x_o)}{y^2 + z^2} \left\{ 1 + \frac{(x - x_o)}{[(x - x_o)^2 + y^2 + z^2]^{\frac{1}{2}}} \right\} dx_o \\ &\quad + a^3 \frac{c}{4\pi \rho U_{\infty}} \frac{\partial}{\partial y} \left( y \int_{-1}^1 \frac{A(x_o)}{y^2 + z^2} \left\{ 1 + \frac{(x - x_o)}{[(x - x_o)^2 + y^2 + z^2]^{\frac{1}{2}}} \right\} dx_o \right) \end{aligned} \quad (48)$$

where  $\bar{P}(x_o)$  and  $A(x_o)$  are to be determined by the matching conditions. Here, the last term is deduced from the last term of Equation (47b). To obtain the inner limit of this expression, we substitute the inner variables and expand for small  $a$ . Then, the following two expansions are obtained:

$$\begin{aligned} 2 \text{ inner (2 outer)} &= U_{\infty} c x + a \left\{ \alpha c Y U_{\infty} \right. \\ &\quad \left. + \frac{Y c}{Y^2 + Z^2} \frac{\partial}{\partial x^2} \int_{-1}^1 \frac{\bar{P}(x_o)}{4\pi \rho U_{\infty}} \frac{(x - x_o)^2}{2} (1 + \text{sgn}(x - x_o)) dx_o \right\} \end{aligned} \quad (49a)$$



and

3 inner (3 outer) =

$$\begin{aligned}
& U_{\infty} c x + a \left\{ U_{\infty} \alpha c Y + \frac{Yc}{Y^2 + Z^2} \frac{\partial^2}{\partial x^2} \int_{-1}^1 \frac{\bar{P}(x_0)}{4\pi\rho U_{\infty}} \frac{(x-x_0)^2}{2} (1 + \operatorname{sgn}(x-x_0)) dx_0 \right. \\
& + \frac{(Z^2 - Y^2)c}{(Z^2 + Y^2)^2} \frac{\partial^2}{\partial x^2} \int_{-1}^1 \frac{A(x_0)}{4\pi\rho U_{\infty}} \frac{(x-x_0)^2}{2} (1 + \operatorname{sgn}(x-x_0)) dx_0 \left. \right\} + a^3 \left\{ \frac{Yc}{4\pi\rho U_{\infty}} \frac{\partial^2}{\partial x^2} c \int_{-1}^1 \bar{P}(x_0) \right. \\
& \operatorname{sgn}(x-x_0) \left[ \frac{1}{4} + \frac{1}{2} \ln |x-x_0| + \frac{1}{2} \ln 2 - \frac{1}{2} \ln \sqrt{Y^2 + Z^2} \right] dx_0 + \\
& \frac{1}{4\pi\rho U_{\infty}} \frac{\partial^2}{\partial x^2} c \int_{-1}^1 A(x_0) \operatorname{sgn}(x-x_0) \left[ \frac{1}{4} \frac{(Z^2 - Y^2)}{(Z^2 + Y^2)} + \frac{1}{2} \ln 2 - \frac{1}{2} \ln \sqrt{Y^2 + Z^2} \right] dx_0 \\
& + a^3 \ln a \left\{ \frac{1}{4\pi\rho U_{\infty}} \frac{\partial^2}{\partial x^2} c \int_{-1}^1 \frac{A(x_0)}{2} \operatorname{sgn}(x-x_0) dx_0 \right. \\
& \left. - Y \frac{1}{4\pi\rho U_{\infty}} \frac{\partial^2}{\partial x^2} c \int_{-1}^1 \frac{\bar{P}(x_0)}{2} \operatorname{sgn}(x-x_0) dx_0 \right\} \quad (49b)
\end{aligned}$$

Matching

Matching the two outer (two inner) to two inner (two outer) [that is, Equations (47a) and (49a)] results in

$$\bar{P}(x) = 2\pi\rho U_{\infty} \left( \frac{\Gamma}{\pi} \lambda h + \frac{1}{2} h^2 U_{\infty} \alpha \right)' \quad (50)$$

where the prime denotes differentiation with respect to  $x$ . Matching two inner (three outer) to three outer (two inner), we obtain

$$A(x) = -2\pi\rho U_{\infty} \left( \frac{\Gamma}{\pi} Y_1 Z_1 \right)' \quad (51)$$

After substitution of these results in Equation (49b), the three inner (three outer) becomes

$$\begin{aligned}
\phi^o \sim U_\infty c x + a \left\{ U_\infty \alpha c Y + \left( \frac{\Gamma \lambda h c}{\pi} + \frac{1}{2} h^2 U_\infty \alpha c \right) \frac{Y}{Y^2 + Z^2} - \frac{\Gamma \alpha Y, Z, c}{\pi} \frac{(Z^2 - Y^2)}{(Z^2 + Y^2)^2} \right\} \\
+ a^3 \left\{ \frac{Y}{4} \left( \frac{\Gamma \lambda h c}{\pi} + \frac{1}{2} h^2 U_\infty \alpha c \right)'' - \frac{(Z^2 - Y^2)}{(Z^2 + Y^2)} \frac{(c \Gamma \alpha Y, Z, c)''}{4} \right. \\
- \left( \frac{\Gamma \lambda c h}{\pi} + \frac{1}{2} h^2 U_\infty \alpha c \right)'' \frac{Y}{2} \ln \sqrt{Y^2 + Z^2} + \left( \frac{\Gamma \lambda c h}{\pi} + \frac{1}{2} h^2 U_\infty \alpha c \right)'' \frac{Y}{2} \ln 2 \\
+ \frac{1}{2} \left( \frac{c \Gamma \alpha}{\pi} Y, Z, c \right)'' \ln \sqrt{Y^2 + Z^2} + \frac{Y}{4} \frac{\partial^2}{\partial x^2} \int_{-1}^1 \left( \frac{\Gamma \lambda c h}{\pi} + \frac{1}{2} h^2 U_\infty \alpha c \right)' \text{sgn}(x - x_0) \ln |x - x_0| dx_0 \\
- \frac{1}{4} \frac{\partial^2}{\partial x^2} \int_{-1}^1 \left( \frac{c \Gamma \alpha}{\pi} Y, Z, c \right)' \text{sgn}(x - x_0) \ln |x - x_0| dx_0 \left. \right\} \\
+ a^3 \ln a \left\{ \frac{1}{2} \left( \frac{\Gamma \alpha}{\pi} Y, Z, c \right)'' - \frac{Y}{2} \left( \Gamma \lambda c h + \frac{1}{2} h^2 U_\infty \alpha c \right)'' \right\} \quad (52)
\end{aligned}$$

We see from Equation (52) that the next inner solution must be of the form

$$a^3 \tilde{\Phi}_{31}^i + a^3 \ln a \tilde{\Phi}_{32}^i$$

where

$$\tilde{\Phi}_{31}^i = \tilde{\Phi}_{31}^i(P) + \tilde{\Phi}_{31}^i(c)$$

where  $\tilde{\Phi}_{31}^i(P)$  is the particular solution of

$$\tilde{\Phi}_{31YY}^i(P) + \tilde{\Phi}_{31ZZ}^i(P) = - \frac{\partial^2}{\partial x^2} \tilde{\Phi}_1^i \quad (53)$$

This equation is solved similarly to Equation (32).

The particular solution is determined to be

$$\begin{aligned}
\Phi_{31}^i(\rho) = R.P. \frac{i\bar{\sigma}}{4} \frac{\partial^2}{\partial x^2} \left\{ U_\infty \alpha c \left[ \frac{\sigma}{2} \sqrt{\sigma^2 - h^2} - \frac{h^2}{2} \cosh^{-1} \frac{\sigma}{h} \right] \right. \\
+ \frac{\Gamma_c}{2\pi} \left[ \sigma \ln \left( \frac{\sqrt{\sigma^2 - h^2} - \sqrt{\sigma_1^2 - h^2}}{\sqrt{\sigma^2 - h^2} + \sqrt{\sigma_1^2 - h^2}} \right) + \sigma_1 \ln 2 \left( \frac{\sigma \sigma_1 + h^2 + \sqrt{\sigma^2 - h^2} \sqrt{\sigma_1^2 - h^2}}{\sqrt{\sigma^2 - h^2} - \sqrt{\sigma_1^2 - h^2}} \right) \right. \\
- \bar{\sigma}_1 \ln 2 \left( \frac{\sigma \bar{\sigma}_1 + h^2 - \sqrt{\sigma^2 - h^2} \sqrt{\sigma_1^2 - h^2}}{\sqrt{\sigma^2 - h^2} + \sqrt{\sigma_1^2 - h^2}} \right) - \sqrt{\sigma_1^2 - h^2} \ln 2 \left( \sigma + \sqrt{\sigma^2 - h^2} \right) \\
\left. \left. - \sqrt{\bar{\sigma}_1^2 - h^2} \ln 2 \left( \sigma + \sqrt{\sigma^2 - h^2} \right) \right] \right\}
\end{aligned} \tag{54}$$

$\Phi_{31}^i(c)$  and  $\Phi_{32}^i$  satisfy Laplace's equation and the boundary condition of no flow through the plate. They are chosen such that the three outer (three inner) expansion matches Equation (52) and the Kutta condition at the leading edge is preserved.

This is found by inspection to be

$$\begin{aligned}
\Phi_{31}^i(c) = R.P. \frac{i}{4} \frac{\partial^2}{\partial x^2} \left\{ \frac{\Gamma_c}{U_\infty} \left[ -\sigma^2 \ln \frac{\sqrt{\sigma^2 - h^2} - \sqrt{\sigma_1^2 - h^2}}{\sqrt{\sigma^2 - h^2} + \sqrt{\sigma_1^2 - h^2}} + \sigma \sigma_1 \ln 2 \left( \frac{\sigma \sigma_1 + h^2 + \sqrt{\sigma^2 - h^2} \sqrt{\sigma_1^2 - h^2}}{\sqrt{\sigma^2 - h^2} - \sqrt{\sigma_1^2 - h^2}} \right) \right. \right. \\
+ \sigma \bar{\sigma}_1 \ln 2 \left( \frac{\sigma \bar{\sigma}_1 + h^2 - \sqrt{\sigma^2 - h^2} \sqrt{\sigma_1^2 - h^2}}{\sqrt{\sigma^2 - h^2} + \sqrt{\sigma_1^2 - h^2}} \right) + \sigma (\sqrt{\sigma_1^2 - h^2} + \sqrt{\bar{\sigma}_1^2 - h^2}) \ln 2 (\sigma + \sqrt{\sigma^2 - h^2}) \left. \right] \\
+ U_\infty \alpha c \left[ -\sigma^2 \sqrt{\sigma^2 - h^2} + \frac{h^2}{2} \sigma \cosh^{-1} \frac{\sigma}{h} \right] \left. \right\} \\
+ \frac{1}{4} R.P. \left( \frac{\Gamma_c Y_1 Z_1}{\pi} \right)'' \ln \left[ (\sqrt{\sigma^2 - h^2} - \sqrt{\sigma_1^2 - h^2})(\sqrt{\bar{\sigma}_1^2 - h^2} + \sqrt{\sigma^2 - h^2}) \right] \\
- 2 Y_1 \bar{Z}_1 - \frac{1}{4} \frac{\partial^2}{\partial x^2} \int_{-1}^1 \frac{(\Gamma_c Y_1 \bar{Z}_1)'}{\pi} \operatorname{sgn}(x - x_0) \ln |x - x_0| dx_0 + G_2(x) \Phi_1^i
\end{aligned} \tag{55}$$

where

$$\begin{aligned}
G_2(x) = & \left( \frac{1}{4} + \frac{1}{2} \ln 2 \right) \left( \frac{\Gamma \lambda}{U_\infty \alpha \pi} + \frac{1}{2} h^2 \right)'' + \frac{1}{4} \frac{\partial^2}{\partial x^2} \int_{-1}^1 \left( \frac{\Gamma \lambda}{U_\infty \alpha \pi} + \frac{1}{2} h^2 \right)' \\
& \operatorname{sgn}(x-x_0) \ln |x-x_0| dx_0 - \frac{1}{2} \left( \frac{h^2}{2} \ln h \right)'' + \frac{1}{2} \frac{1}{U_\infty \alpha c} \frac{\lambda''}{\pi} \ln 4 + \frac{1}{4} (h^2)'' \\
& + \frac{1}{4\alpha} R.P. \frac{\partial^2}{\partial x^2} \left\{ \frac{\Gamma c}{2\pi U_\infty} \left( -4\lambda + 2\sigma_i \ln 2(\sigma_i + \sqrt{\sigma_i^2 - h^2}) - 2\bar{\sigma}_i \ln 2(\bar{\sigma}_i - \sqrt{\bar{\sigma}_i^2 - h^2}) \right) \right\} \quad (56)
\end{aligned}$$

Then,  $\Phi_{31}^i$  is

$$\begin{aligned}
\Phi_{31}^i = & R.P. \frac{i}{4} \frac{\partial^2}{\partial x^2} \left\{ \frac{\Gamma c}{2\pi} \left[ \sigma(\bar{\sigma} - \sigma) \ln \frac{\sqrt{\sigma^2 - h^2} - \sqrt{\sigma_i^2 - h^2}}{\sqrt{\sigma^2 - h^2} + \sqrt{\sigma_i^2 - h^2}} \right. \right. \\
& + \sigma_i(\bar{\sigma} - \sigma) \ln 2 \left( \frac{\sigma\sigma_i + h^2 + \sqrt{\sigma^2 - h^2} \sqrt{\sigma_i^2 - h^2}}{\sqrt{\sigma^2 - h^2} - \sqrt{\sigma_i^2 - h^2}} \right) - \bar{\sigma}_i(\bar{\sigma} - \sigma) \ln 2 \left( \frac{\sigma\bar{\sigma}_i + h^2 - \sqrt{\sigma^2 - h^2} \sqrt{\bar{\sigma}_i^2 - h^2}}{\sqrt{\sigma^2 - h^2} + \sqrt{\bar{\sigma}_i^2 - h^2}} \right) \\
& \left. \left. - (\bar{\sigma} - \sigma)(\sqrt{\bar{\sigma}_i^2 - h^2} + \sqrt{\bar{\sigma}_i^2 - h^2}) \ln 2(\sigma + \sqrt{\sigma^2 - h^2}) \right] + U_\infty \alpha c \left[ \sigma(\bar{\sigma} - \sigma) \sqrt{\sigma^2 - h^2} - \frac{h^2}{2} (\bar{\sigma} - \sigma) \cosh^{-1} \frac{\sigma}{h} \right] \right\} \\
& + \frac{1}{4} R.P. \left( \frac{\Gamma c Y_1 \bar{Z}_1}{\pi} \right)'' \ln \left[ \left( \sqrt{\sigma^2 - h^2} - \sqrt{\sigma_i^2 - h^2} \right) \left( \sqrt{\sigma^2 - h^2} + \sqrt{\bar{\sigma}_i^2 - h^2} \right) \right] \\
& - 2Y_1 \bar{Z}_1 - \frac{1}{4} \frac{\partial^2}{\partial x^2} \int_{-1}^1 \frac{(\Gamma c Y_1 \bar{Z}_1)'}{\pi} \operatorname{sgn}(x-x_0) \ln |x-x_0| dx_0 + G_2(x) \Phi_1^i \quad (57)
\end{aligned}$$

and

$$\begin{aligned}
\Phi_{32}^i = & \frac{1}{2} \left( \frac{\Gamma c Y_1 \bar{Z}_1}{\pi} \right)'' - G_3(x) \Phi_1^i \\
G_3(x) = & \frac{1}{2} \left( \frac{\Gamma \lambda}{U_\infty \pi} + \frac{1}{2} h^2 \right)'' \quad (58)
\end{aligned}$$

### Results

Again, as in the unseparated flow case, the terms in  $\Phi_{31}^i$  containing  $(\bar{\sigma} - \sigma)$  do not contribute to the lift and Blasius' theorem may be used to calculate lift. This results in the following expressions

$$C_L = \frac{2\pi a}{5} \left( \frac{1}{2} + \lambda^2 + \tau^2 \right) \left( 1 + a^2 G_2(1) - a^2 \ln a G_3(1) \right) \quad (59a)$$

and the corresponding loading is

$$\begin{aligned} \frac{\bar{P}(x)}{\frac{1}{2}\rho U_\infty^2 c} = 2\pi a \left( \frac{h^2}{2} + \lambda^2 + \tau^2 \right)' \left( 1 + a^2 G_2(x) - a^2 \ln a G_3(x) \right) \\ + 2\pi a^3 \left( \frac{h^2}{2} + \lambda^2 + \tau^2 \right) \left( G_2'(x) - \ln a G_3'(x) \right) \end{aligned} \quad (59b)$$

The factor  $\frac{2\pi a}{\bar{S}} \left( \frac{1}{2} + \lambda^2 + \tau^2 \right)$  appearing in Equation (59a) is recognized as the lift coefficient as evaluated from the Brown and Michael analysis with

$$\bar{S} = \int_{-1}^1 h(x) dx.$$

Again,  $G_2(x)$  contains an integral of the type given in Equation (41). Unfortunately, the first-order loading for the separated flow case, Equation (50), is of such a form that the requirements on  $h$  cannot be derived explicitly. However, in view of the results obtained for the unseparated flow case, we can expect reasonable results only for the gothic wing. Therefore, this was the only planform for which numerical results were obtained. Since the vortex strength and position are implicit functions of  $\alpha$  as well as  $x$ ,  $G_2(1)$  and  $G_3(1)$  are also implicit functions of  $\alpha$  and Equation (59) must be evaluated numerically for  $C_L$ . Results have been obtained for an aspect-ratio-one gothic wing with  $h = \frac{1}{4}(3+2x-x^2)$  and are presented in Figure 6. Again, the "finite-part concept" was used to evaluate the integral in  $G_2(1)$ . It is seen that the present results offer a significant improvement over the first-order Brown and Michael theory but are still somewhat higher than the experimental results.

## DISCUSSION OF RESULTS AND CONCLUSIONS

A second-order, slender-wing theory has been developed for incompressible flow about slender wings with and without leading-edge separation. The theory applies to wings that have sufficiently smooth planform shapes. For planforms such as the gothic which satisfy the smoothness requirements, the inclusion of second-order aspect-ratio effects results in a significant improvement over first-order theory in the prediction of lift. For a gothic wing of aspect ratio 1.0, the second-order theory predicts values of lift that agree closely with the experimental results up to an angle of attack of approximately twelve degrees. This agreement was obtained even though the separated flow effects were represented by the very simple cross-flow model of Brown and Michael (Reference 2).

Furthermore, the improved lift prediction for the gothic wing was obtained even though the separated flow model was not required to satisfy the Kutta condition at the trailing edge. Only the first-order unseparated flow model happens to meet this condition for the gothic planform. Therefore, the improvement in the theory for the separated flow case must be attributed to the inclusion of second-order aspect-ratio effects.

The delta planform does not have the required smoothness at the trailing edge and so not even the unseparated first-order model satisfies the Kutta condition in this case. The second-order theory fails to produce any improvement in the prediction of lift for unseparated flow over a delta wing. This failure is attributed to the nonuniformity of the first-order (i. e., the conventional slender-wing) theory at the trailing edge. Before a higher-order theory which will be valid for delta-wing planforms can be developed, the first-order flow model must be modified to eliminate the nonuniformity at the trailing edge, at least in the unseparated case.

In view of the failure of the second-order theory for delta wings in unseparated flow, this development was not pursued further for application to the separated flow case.

A new cross-flow model for the slender-wing problem was investigated. The model consisted of a double logarithmic spiral with a vortex and a sink located at its core. The model was patterned after the single logarithmic spiral solution obtained by Drasky in Reference 11. The double spiral solution proves to be inadequate for the slender-wing, cross-flow problem because it cannot satisfy the appropriate boundary conditions on the vortex sheet.

## REFERENCES

1. Legendre, R. E'coulement au Voisinage de la Pointe Avant D'une Aile A'forte Fle'che Aux Incidences Mayennu La Recherche Ae'ronautique (ONERA) Report 30 November - December 1952.
2. Brown, C. E. and Michael, Jr., W. H. On Slender Delta Wings with Leading-Edge Separation NACA TN-3430 April 1965.
3. Mangler, K. W. and Smith, J. H. B. Calculation of the Flow Past Slender Delta Wings with Leading Edge Separation RAE Report Aero 2593 May 1957.
4. Smith, J. H. B. Improved Calculations of Leading-Edge Separation from Delta Wings RAE TR 66070 March 1966.
5. Peckham, D. H. Low Speed Wind Tunnel Tests on a Series of Uncambered Slender Pointed Wings with Sharp Edges ARC R&M 3168 December 1958.
6. Bergesen, A. J. and Porter, J. D. An Investigation of the Flow Around Slender Delta Wings with Leading Edge Separation Princeton University Department of Aeronautical Engineering Report 510 May 1960.
7. Lemaire, D. A. Some Observations of the Low-Speed Flow Over a Sharp-Edged Delta Wing of Unit Aspect Ratio Department of Supply Australian Defense Scientific Service Aeronautical Research Laboratories Report ARL/A 126 January 1965.
8. Wentz, Jr., N. H. and McMahon, M. C. An Experimental Investigation of the Flow Fields About Delta and Double Delta Wings at Low Speeds NASA Contractor Report CR 521 August 1966.
9. Polhamus, E. C. A Concept of the Vortex Lift of Sharp-Edge Delta Wings Based on a Leading-Edge Suction Analogy NASA TND-3767 December 1966.
10. Wang, K. C. A New Approach to "Not-So-Slender" Wing Theory Journal of Mathematics and Physics Vol XLVII No. 4 December 1968.
11. Drasky, J. On Some Particular Cases of the Solution of Laplace's Equation Describing the Principal Properties of Vortex Formation in Fluids Lietschrift fur angewandte Mathematik and Mechanik Vol 46 March 1966.

12. Lagerstrom, P. A., Howard, L. N., and Liu, C. S. (Editors) Fluid Mechanics and Singular Perturbations A Collection of Papers by Saul Kaplun Academic Press Inc. 1967.
13. Van Dyke, M. Perturbation Methods in Fluid Mechanics Academic Press 1964.
14. Martin, E. D. A Method of Asymptotic Expansions for Singular Perturbation Problems With Application to Viscous Flow NASA TND-3899 April 1967.
15. Van Dyke, M. Lifting-Line Theory as a Singular-Perturbation Problem Stanford University Report SUDAER 165 August 1963.
16. Jones, R. T. Properties of Low-Aspect-Ratio Pointed Wings at Speeds Below and Above the Speed of Sound NACA Report 835 1946.
17. Broderick, J. B. Supersonic Flow Round Pointed Bodies of Revolution Quarterly Journal of Mechanics and Applied Mathematics 2 1949 pp. 98 - 120.
18. Lighthill, M. J. Supersonic Flow Past Slender Pointed Bodies of Revolution at Yaw Quarterly Journal of Mechanics and Applied Mathematics 1 1948 pp. 76 - 89.
19. Ashley, H. and Landahl, M. Aerodynamics of Wings and Bodies Addison-Wesley Publication Company, Inc. 1965.
20. Adams, M. C. and Sears, W. R. Slender Body Theory - Review and Extension JAS 1953 pp. 85 - 98.
21. Mangler, K. W. Improper Integrals in Theoretical Aerodynamics ARC R&M 2424.
22. Friedman, B. Techniques of Applied Mathematics Theory of Distributions New York University Mathematics Research Group Research Report EM-47 October 1952.
23. Smith, J. H. B. A Theory of the Separated Flow From the Curved Leading of a Slender Wing RAE Technical Note Aero 2535 November 1957.
24. Jobe, C. E. An Aerodynamic Theory of Slender Wings With Leading Edge Separation A Thesis Ohio State University 1966.
25. Hildebrand, F. B. Introduction to Numerical Analysis McGraw-Hill Book Company, Inc. 1956 pp. 236 - 237.
26. Alexander, R. C. Self-Similar Hydrodynamics With Vortex Sheets AFOSR Scientific Report 65-0642.



## APPENDIX A

### Drasky Flow Model

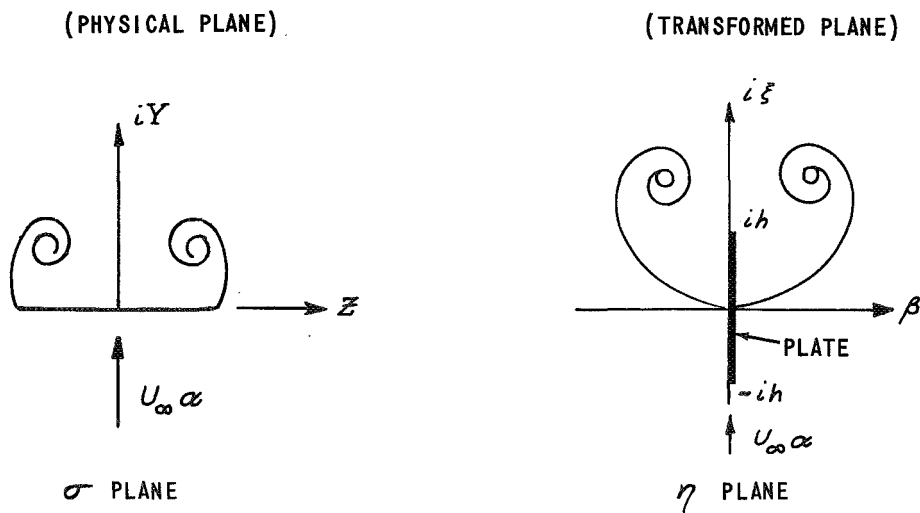
An analytic solution for the cross flow is desired for use in the matched asymptotic expansion analysis of the separated flow case.

It appeared that a fundamental solution developed by Drasky (Reference 11) for a two-dimensional nonsteady logarithmic spiral vortex sheet with a concentrated vortex and a sink located at its core could serve as a basis for the desired solution. Drasky's solution for the complex velocity potential is of the form

$$W(\eta) = C(t) (\eta - \tilde{q})^{\frac{1}{2} - i\sqrt{\frac{3}{2}}} - \frac{(\Gamma(t) + i\phi(t)) \ln(\eta - \tilde{q})}{2\pi} \quad (A-1)$$

where  $\eta$  is the complex variable. Such solutions have also been studied in a more general sense by Alexander (Reference 26).

If we let  $\sigma$  be the complex variable in the physical plane, then the cross-flow problem for the separated-flow, slender-wing case is most easily analyzed in the transformed  $\eta$  plane where  $\eta^2 = \sigma^2 - h^2$ . This transformation transforms the plate into the vertical  $\eta$  axis and the resulting flow is sketched below.



The advantage of this transformation is that a solution symmetric about the  $\xi$  axis automatically satisfies the condition of no flow through the plate.

A study of References 11 and 26 indicates that the desired solution in the  $\eta$  plane should be of form

$$W(\eta) = F_1(\eta) + F_2(\eta) \quad (\text{A-2a})$$

where

$$F_1(\eta) = C_2(\eta - \tilde{q})^{\frac{1}{2} + i\sqrt{\frac{3}{2}}} (\eta + \tilde{q})^{\frac{1}{2} - i\sqrt{\frac{3}{2}}}, \quad (\text{A-2b})$$

$$F_2(\eta) = \frac{\Gamma - iQ}{2\pi i} \ln(\eta - \tilde{q}) - \frac{\Gamma + iQ}{2\pi i} \ln(\eta + \tilde{q}) + C_1. \quad (\text{A-2c})$$

Here,  $F_1(\eta)$  represents the complex potential of the spiral sheets and  $F_2(\eta)$  represents the complex potential of the concentrated singularities located at the spiral cores at  $\tilde{q}$  and  $-\tilde{q}$ .  $\Gamma, Q, \tilde{q}, C_1, C_2$  are functions of  $\chi$  to be determined. The conditions available to determine these functions are:

1. There is no flow through the plate or vortex sheet.  
The sheet and plate are stream surfaces.
2. There is no pressure jump across the vortex sheet.
3. The loading at the edge of the plate is zero (Kutta condition).

We then assume that the inner solution expands as

$$\Phi^i \sim \Phi_0^i + a^2 \Phi_1^i \quad (\text{A-3})$$

where  $\Phi_1^i$  is of the form of Equation (A-2). In order to generate the correct first-order conditions on the vortex sheet, it is found that the first gage function must be  $a^2$ . Since the analysis is performed in the transformed  $\eta$  plane, the requirement of no flow through the plate need not be considered further.

If the vortex sheet is given by  $\mathcal{S}(Y, Z; X) = 0$ , the exact stream surface requirement on the sheet can be specified by

$$\nabla \Phi \cdot \nabla \mathcal{S} = 0; \quad (\text{on sheet}) \quad (\text{A-4})$$

where  $\nabla$  is the vector differential operator

$$\nabla \equiv i \frac{\partial}{\partial x} + j \frac{\partial}{\partial y} + k \frac{\partial}{\partial z}.$$

Substituting Equation (A-3) into Equation (A-4) and retaining only the leading terms in  $a$ , Equation (A-4) reduces to

$$U_{\infty} \phi_X + \phi_{,Y}^i \phi_Y + \phi_{,z}^i \phi_{,z}^i = 0 ; \quad (\text{on sheet}). \quad (\text{A-5})$$

The pressure may be calculated from the Bernoulli's equation as

$$-\frac{2P}{\rho} = \nabla \phi \cdot \nabla \phi. \quad (\text{A-6})$$

The approximated form of the pressure jump condition on the sheet is then

$$\Delta \left( -\frac{2P}{\rho} \right) = \Delta \left[ 2U_{\infty} \phi_{,X}^i + \phi_{,Y}^{i,2} + \phi_{,z}^{i,2} \right] = 0 ; \quad (\text{on sheet}) \quad (\text{A-7})$$

Here,  $\Delta$  means jump across the sheet. Equations (A-7) and (A-5) are the conditions derived by Smith (Reference 4).

The leading-edge Kutta condition is most easily applied by requiring that the origin of the transformed plane be a stagnation point or

$$\left. \frac{dW}{d\eta} \right|_{\eta=0} = 0. \quad (\text{A-8})$$

Matching requirements would determine  $C_2$  as

$$C_2 = -iU_{\infty} \left( \frac{\alpha}{a} \right).$$

Drasky locates the sheet  $\mathcal{S}$  by making the zero streamline of  $F_1$  a branch cut. If we let

$$\begin{aligned} \sigma - \tilde{q} &= r_1 e^{i\theta_1} \\ \sigma + \tilde{q} &= r_2 e^{i\theta_2} \end{aligned}$$

we find that  $\mathcal{S}$  is given by

$$\mathcal{S} = \sqrt{3} \ln \frac{r_1}{r_2} + \theta_1 + \theta_2 - \pi = 0. \quad (\text{A-9})$$

If we let  $\tilde{q} = r_b e^{i\theta_b}$ , the Kutta condition [Equation (A-8)] results in the following two relations:

$$\theta_b = 60^\circ \quad (\text{A-10})$$

and

$$\Gamma = \sqrt{3} Q. \quad (\text{A-11})$$

This last condition unfortunately also makes the zero streamlines of  $F_1$  and  $F_2$  coincide so that

$$\Phi'_{1Y} \mathcal{J}_Y + \Phi'_{1Z} \mathcal{J}_Z = 0; \quad (\text{on sheet}) \quad (\text{A-12})$$

which has been verified through substitution. Insertion of Equation (A-12) in Equation (A-5) gives

$$\mathcal{J}_X = 0 \quad (\text{A-13})$$

This indicates that the sheet shape is not a function of  $x$  which is a physically unacceptable result.

We may rearrange Equations (A-5) and (A-7) into the following forms:

$$\frac{\Phi'_{1Y} \mathcal{J}_Y + \Phi'_{1Z} \mathcal{J}_Z}{\mathcal{J}_X} = -U_\infty; \quad (\text{on sheet}) \quad (\text{A-14})$$

$$\frac{\Delta[\Phi'^2_{1Y} + \Phi'^2_{1Z}]}{\Delta\Phi'_{1X}} = -2U_\infty; \quad (\text{on sheet}). \quad (\text{A-15})$$

The functional requirement on  $\Phi'_i$  and  $\mathcal{J}$  can be imposed that they must combine so that the left-hand side of both Equations (A-14) and (A-15) are either nonzero constants or are, at most, functions of  $X$  only (that is, no  $Z$  or  $Y$  dependency). Examination of Equations (A-2) and (A-9) show that they do not meet this functional requirement for Equation (A-15). Therefore, we conclude that a  $\Phi'_i$  of the form of Equation (A-2) and  $\mathcal{J}$  as given by Equation (A-9) do not comprise a satisfactory solution for the posed cross-flow problem.

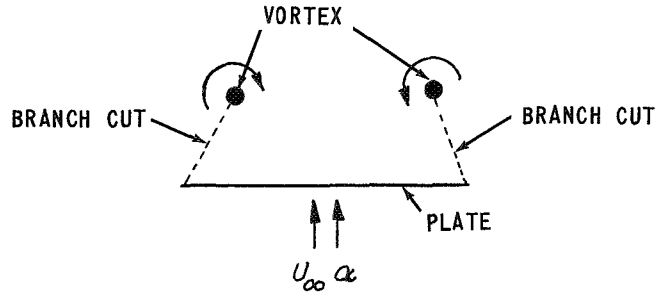
Two modifications to this solution were also considered. First, the sink was removed from Equation (A-2) (i. e.,  $Q=0$ ). It was found that such a solution cannot satisfy the leading-edge Kutta condition. Second, the sheet shape was modified by making the spiral lead angle a function of  $(X)$ . However, no shape has been found that satisfies the functional requirements of Equations (A-14) and (A-15).

The basic failings of this flow model apparently result from application of the leading-edge Kutta condition [Equation (A-8)] which was not a constraint considered by Drasky (Reference 11). The Drasky model was not pursued further. However, we believe that it merits further consideration and should not be dismissed as having no potential applicability. The features of this model appear to be so similar to the essential characteristics of the physical situation that, we believe, only minor modifications could produce a highly satisfactory mathematical model.

## APPENDIX B

### Brown and Michael Flow Model

The Brown and Michael flow model and the method used to calculate the first-order solutions for the gothic and cambered wings are outlined here for convenience and completeness. In the Brown and Michael flow model, each spiral vortex sheet is represented by a concentrated vortex and a branch cut which connects the vortex and the leading edge. The resulting cross-flow model is indicated in the following sketch.



The complex potential for such a cross flow is

$$W = -i \left\{ U_\infty \alpha \sqrt{\sigma^2 - h^2} + \frac{\Gamma}{2\pi} \ln \frac{\sqrt{\sigma^2 - h^2} - \sqrt{\sigma_1^2 - h^2}}{\sqrt{\sigma^2 - h^2} + \sqrt{\sigma_1^2 - h^2}} \right\}$$

where  $\Gamma$  is the strength of the vortices located at  $\sigma_1$  and  $\bar{\sigma}_1$  and all three quantities are to be determined.

In this flow model, the local pressure jump and stream surface conditions cannot be applied on the sheet. They are replaced by an overall force balance on the branch cut and concentrated vortex. The force balance plus the leading-edge Kutta condition then provide sufficient conditions to determine  $\Gamma$  and  $\sigma_1$ .

In this flow model, the branch cut can be considered as a vortex sheet composed of vorticity aligned perpendicular to the free stream with the strength of the sheet being only a function of  $x$ . The Helmholtz laws then give the strength of this sheet as  $\frac{d\Gamma}{dx}$ . The Kutta-Joukowski theorem can be used to calculate the force on the sheet and vortex.

The force on the sheet  $F_s$  per unit depth is

$$F_s = i \rho U_\infty \frac{d\Gamma}{dx} (\sigma_1 - h).$$

The force on the vortex  $F_V$  per unit depth is

$$F_V = -i\rho\Gamma \left( \frac{dW_1}{d\sigma} \Big|_{\sigma_1} - U_\infty \frac{d\sigma_1}{dx} \right)$$

where  $\frac{dW_1}{d\sigma} \Big|_{\sigma_1}$  is the complex velocity evaluated at  $\sigma_1$  excluding the contribution from the vortex located at  $\sigma_1$ . The force balance condition then gives

$$\rho U_\infty \frac{d\Gamma}{dx} (\sigma_1 - h) = \rho\Gamma \left( \frac{dW_1}{d\sigma} \Big|_{\sigma_1} - U_\infty \frac{d\sigma_1}{dx} \right). \quad (\text{B-1})$$

The leading-edge Kutta condition is

$$2\pi U_\infty \alpha = \Gamma \left( \frac{1}{\sqrt{\sigma_1^2 - h^2}} + \frac{1}{\sqrt{\bar{\sigma}_1^2 - h^2}} \right). \quad (\text{B-2})$$

For conical flow where the unknowns can be considered as linearly proportional to  $x$ , Equations (B-1) and (B-2) represent a system of nonlinear algebraic equations which can be solved numerically for the constants of proportionality. This was done in the original paper by Brown and Michael (Reference 2).

For nonconical flow, Equations (B-1) and (B-2) represent a system of coupled ordinary differential equations and can be used as a continuation scheme to numerically calculate the flow field once sufficient initial conditions are given at an  $x$  station. This has been done by Smith in Reference 23 for curved leading edges and by Jobe in Reference 24 for curved leading edges and camber.

If we let  $\frac{\sigma_1}{h} = \eta + i\xi$  and  $S = ach$ , then Equations (B-1) and (B-2) can be manipulated into the forms

$$\frac{d\eta}{dx} = \frac{C^*(1 + B^*\xi) - B^*D^*(\eta - 1)}{1 + A^*(\eta - 1) + B^*\xi} \quad (\text{B-3})$$

$$\frac{d\xi}{dx} = \frac{D^*[1 + A^*(\eta - 1)] - C^*A^*\xi}{1 + A^*(\eta - 1) + B^*\xi} \quad (\text{B-4})$$

where

$$A^* = \frac{G(\lambda^2 - \tau^2) + 2\lambda\tau H}{\lambda(\lambda^2 + \tau^2)^2(\eta^2 + \xi^2)}$$

$$B^* = \frac{2\tau G\lambda - H(\lambda^2 - \tau^2)}{\lambda(\lambda^2 + \tau^2)^2(\eta^2 + \xi^2)}$$

$$C^* = \frac{\alpha(\chi)}{2\lambda S(\xi^2 + \eta^2)} \left[ \frac{2\lambda H}{\lambda^2 + \tau^2} - \frac{H}{2\lambda} - \frac{N}{2(\lambda^2 + \tau^2)(A^2 + B^2)^2} \right] - (2\eta - 1) \frac{S'}{S} - (\eta - 1) \frac{\alpha'}{\alpha}$$

$$D^* = \frac{\alpha(\chi)}{2\lambda S(\xi^2 + \eta^2)} \left[ \frac{2\lambda G}{\lambda^2 + \tau^2} - \frac{G}{2\lambda} - \frac{M}{2(\lambda^2 + \tau^2)(A^2 + B^2)^2} \right] - 2\xi \frac{S'}{S} - \xi \frac{\alpha'}{\alpha}$$

$$A = \left\{ (\lambda^2 - \tau^2 + 1)^2 + 4\lambda^2 \tau^2 \right\}^{\frac{1}{4}} \sin \theta_4$$

$$B = \left\{ (\lambda^2 - \tau^2 + 1)^2 + 4\lambda^2 \tau^2 \right\}^{\frac{1}{4}} \cos \theta_4$$

$$G = (\eta^2 + \xi^2)(\lambda A + \tau B)$$

$$H = (\eta^2 + \xi^2)(B\lambda - A\tau)$$

$$M = (\lambda G + H\tau)(A^2 - B^2) + 2AB(\lambda H - \tau G)$$

$$N = (\lambda H - \tau G)(A^2 - B^2) - 2AB(\lambda G + \tau H)$$

$$\lambda = \left\{ (\eta^2 - \xi^2 - 1)^2 + 4\eta^2 \xi^2 \right\}^{\frac{1}{4}} \cos \theta_5$$

$$\tau = \left\{ (\eta^2 - \xi^2 - 1)^2 + 4\eta^2 \xi^2 \right\}^{\frac{1}{4}} \sin \theta_5$$

$$\theta_4 = \frac{1}{2} \tan^{-1} \frac{2\lambda\tau}{\lambda^2 - \tau^2 - 1}$$

$$\theta_5 = \frac{1}{2} \tan^{-1} \frac{2\xi\eta}{\eta^2 - \xi^2 - 1}$$

The initial or starting conditions  $\eta_0$  and  $\xi_0$  are obtained by assuming that the flow is conical in the immediate vicinity of the apex. An approximate expression for the conical solution is given in Reference 24 as:

$$\xi_0 = -0.03038 \left( \frac{\alpha x}{s} \right)^2 + 0.28057 \left( \frac{\alpha x}{s} \right) - 0.00451$$

$$\eta_0 = -1.78322 \xi_0^3 + 2.29481 \xi_0^2 - 0.98407 \xi_0 + 0.99031.$$

Equations (B-3) and (B-4) have been integrated down the chord by use of a fourth-order Runge-Kutta method which is given in Reference 25. Once  $\xi$  and  $\eta$  and, hence,  $\lambda$  and  $\tau$  are known as functions of position, the vortex strength is determined from the Kutta condition as

$$\Gamma = \pi \alpha \frac{\lambda^2 + \tau^2}{\lambda} s$$

and the integrated lift to any chord station can be obtained from Blasius' theorem as

$$L(x) = \pi \alpha s^2 \left[ \frac{1}{2} + (\lambda^2 + \tau^2) \right].$$

The above procedure has been programed for a digital computer.



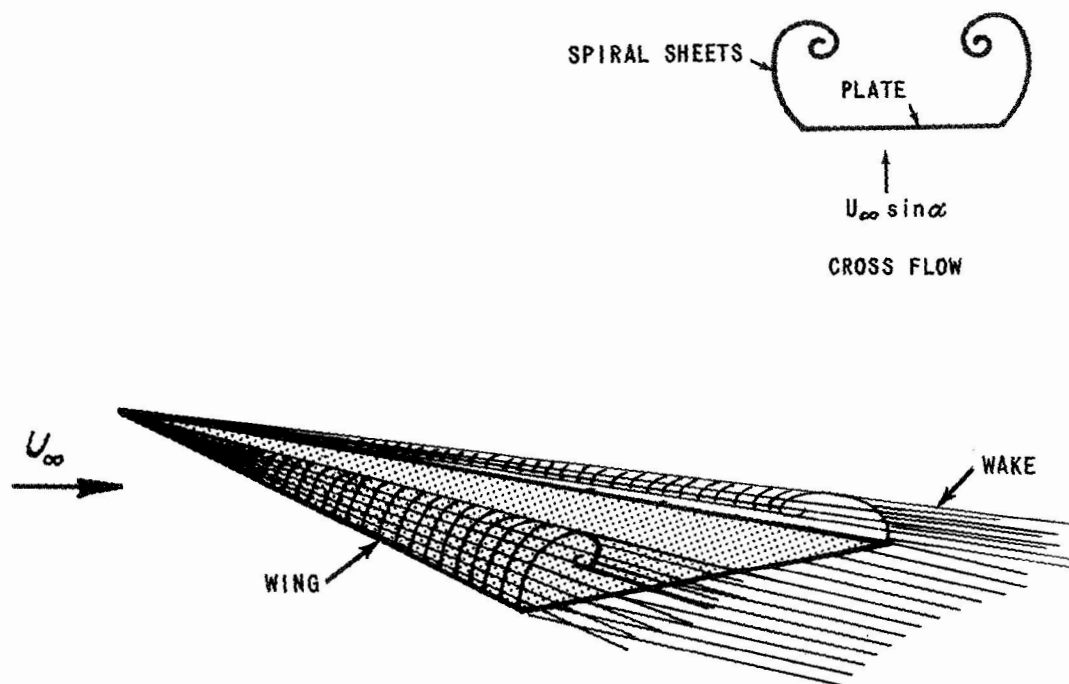


Figure 1 FLOW MODEL WITH SIDE EDGE SEPARATION

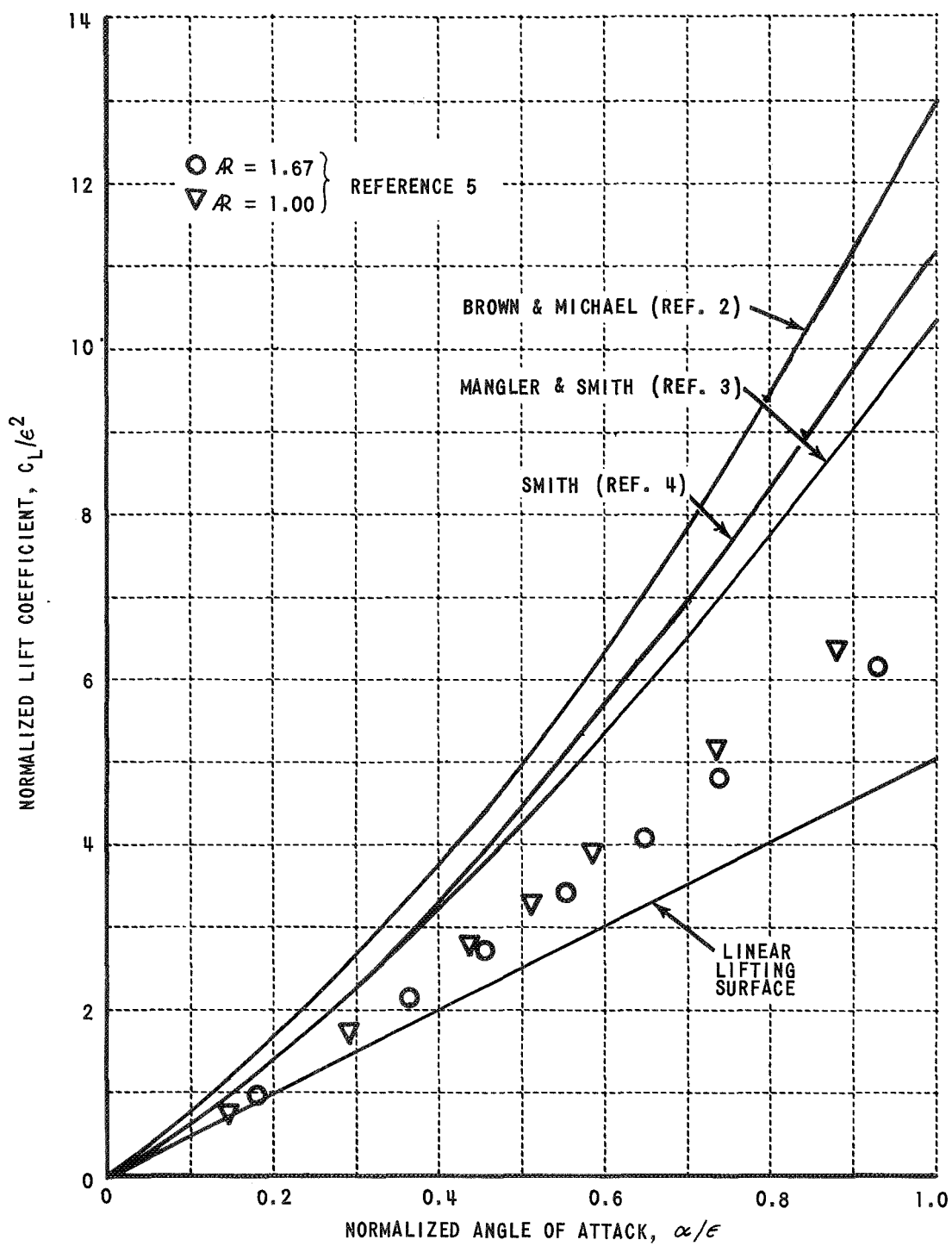


Figure 2 LIFT OF DELTA WINGS AT LOW SPEEDS

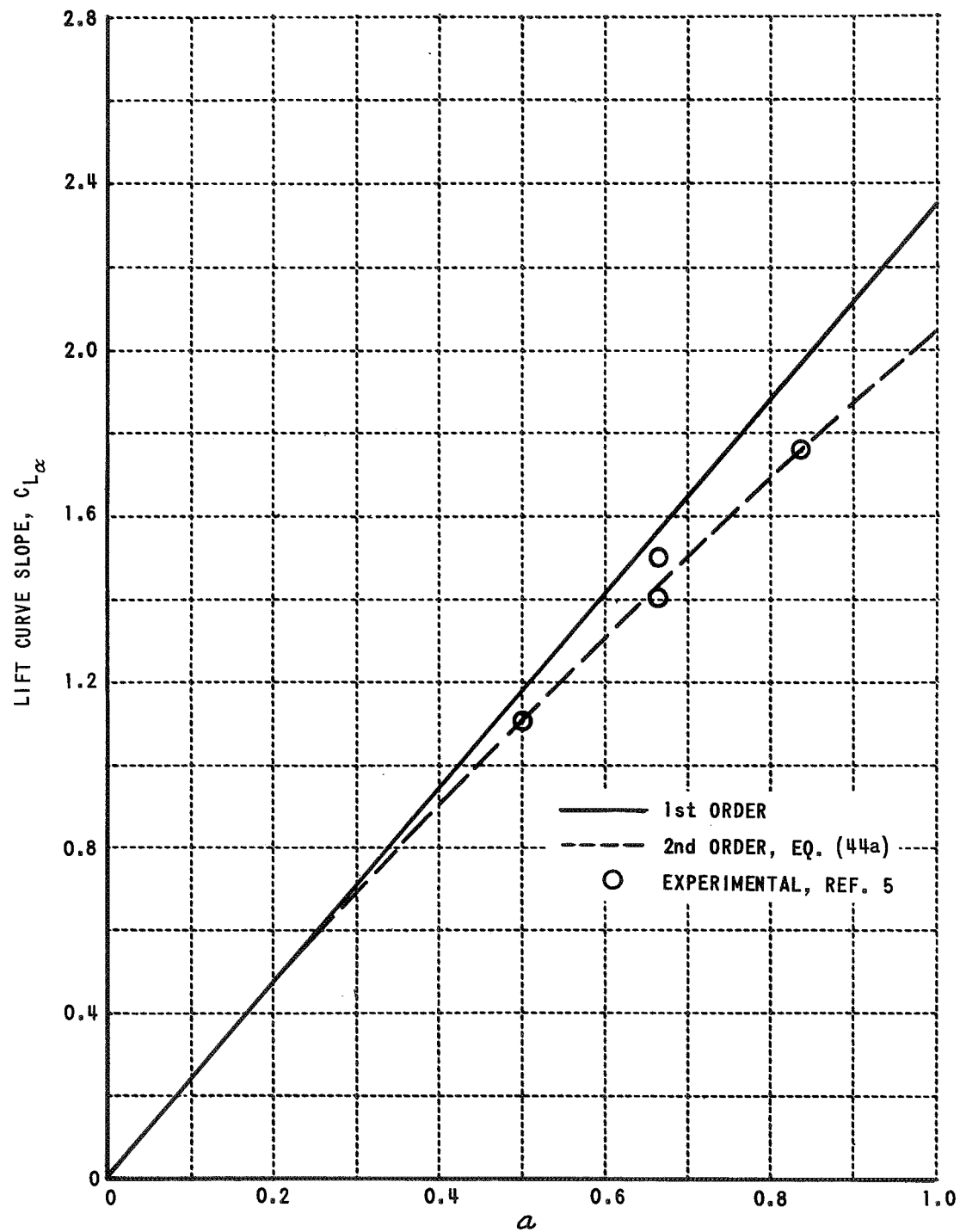


Figure 3 LIFT FOR GOTHIC WINGS  $h = \frac{1}{4} (3 + 2x - x^2)$

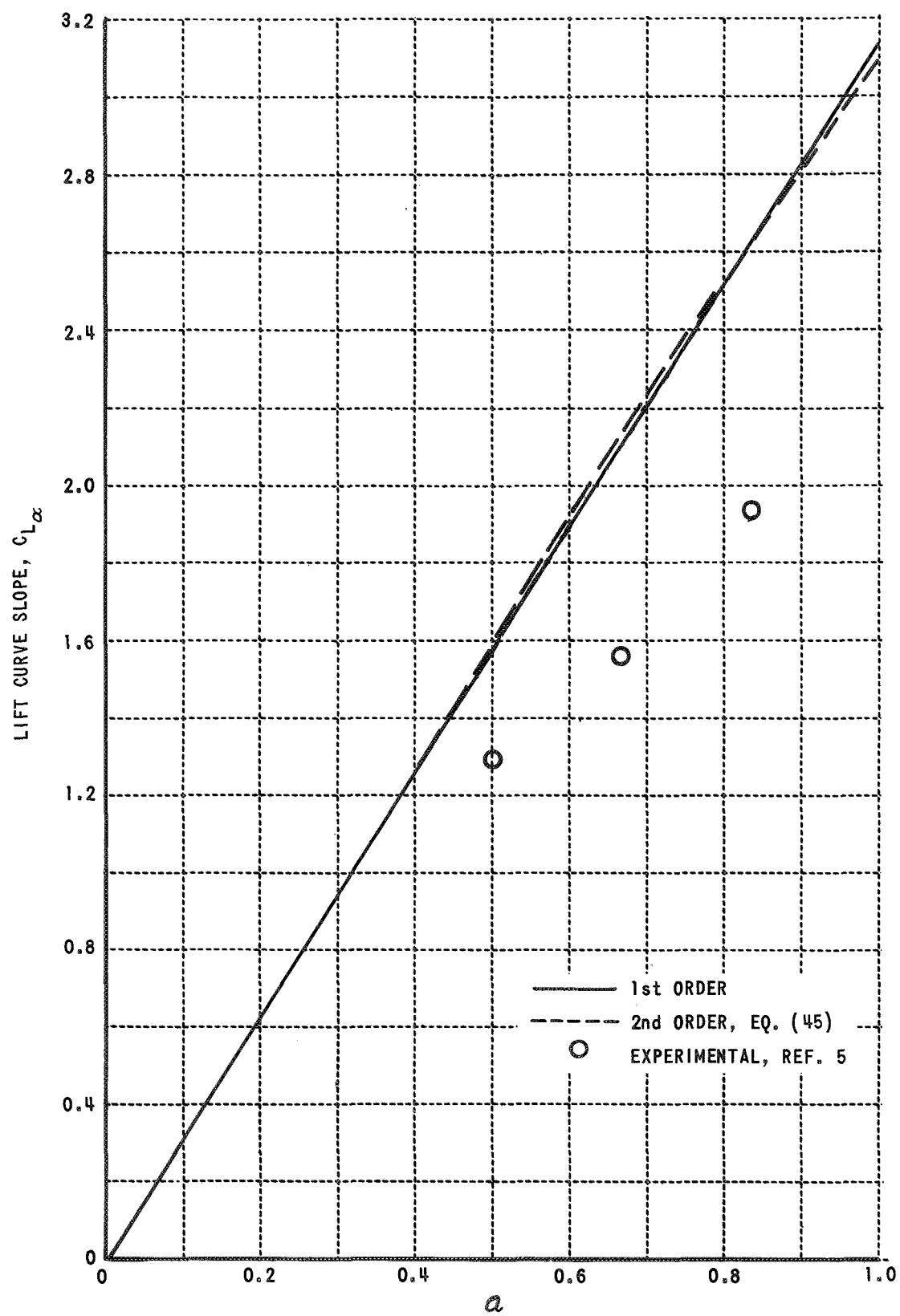


Figure 4 LIFT FOR DELTA WINGS  $h = \frac{1}{2} (1 + x)$

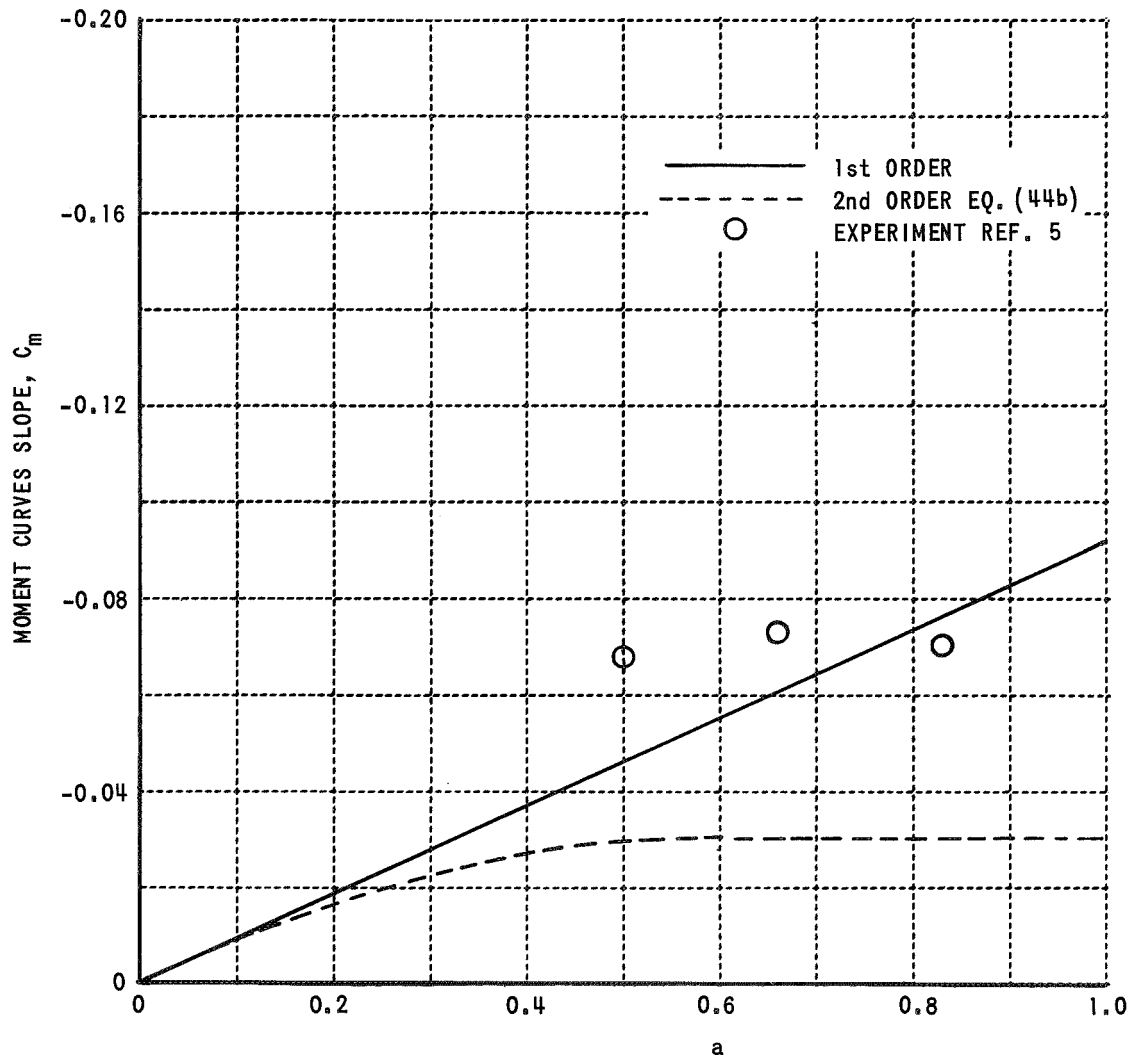


Figure 5 PITCHING MOMENTS FOR GOTHIC WING,  $h = \frac{1}{4}(3+2x-x^2)$

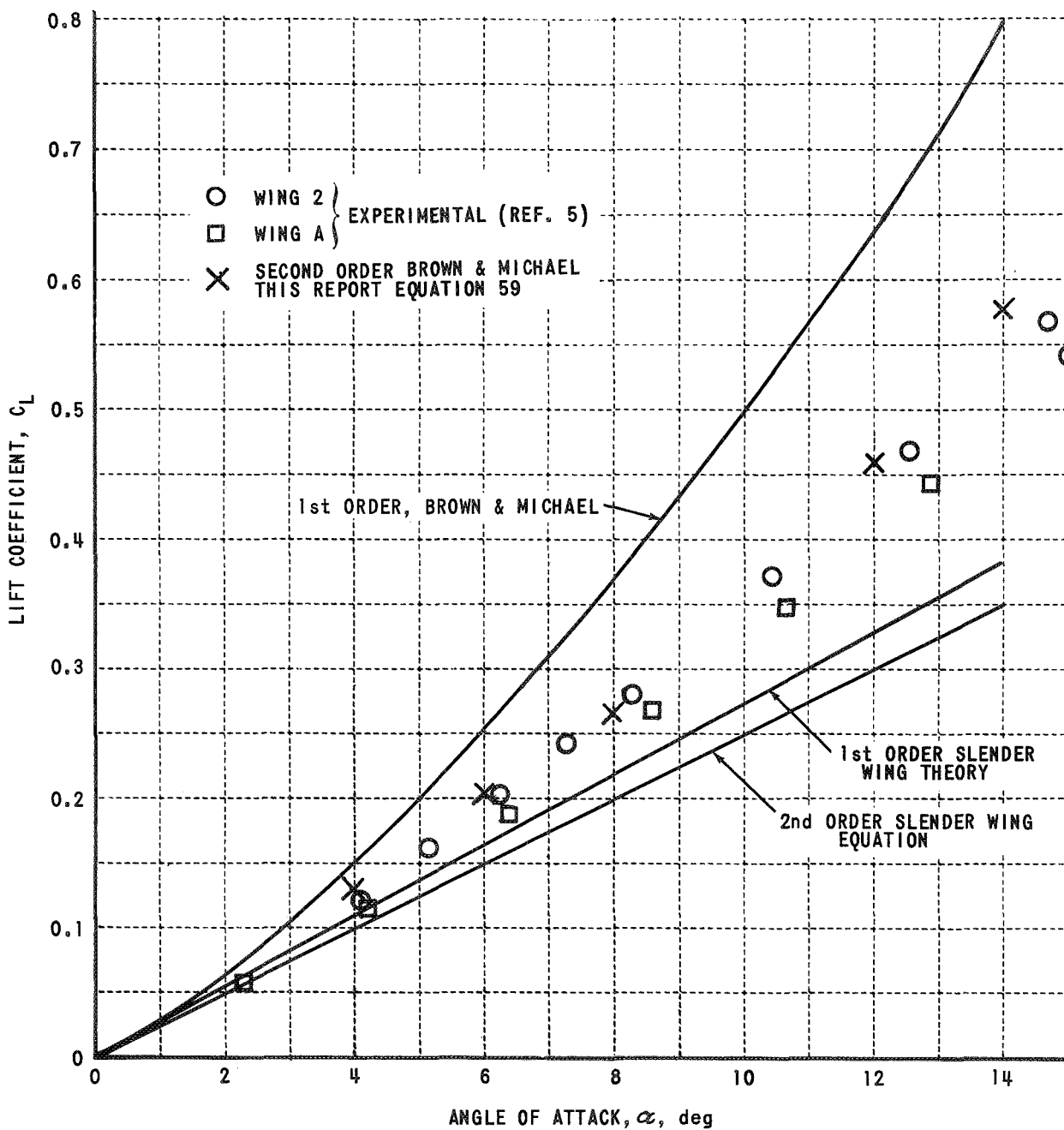


Figure 6 COMPARISON OF EXPERIMENTAL AND THEORETICAL RESULTS FOR AN ASPECT-RATIO-1 GOTHIC WING

# DISTRIBUTION LIST

	<u>Copies</u>
NASA Langley Research Center	
Langley Station	
Hampton, Virginia 23365	
Attention: Research Program Records Unit, Mail Stop 122	1
Raymond L. Zavasky, Mail Stop 117	1
Edward C. Polhamus, Mail Stop 404A	5
John E. Lamar, Mail Stop 404A	1
Percy J. Bobbitt, Mail Stop 245	1
Charles H. Fox, Jr., Mail Stop 404A	1
William B. Kemp, Jr., Mail Stop 404A	1
NASA Ames Research Center	
Moffett Field, California 94035	
Attention: Library, Stop 202-3	1
Mark W. Kelly, Stop 221-2	1
Siegfried N. Wagner, Stop 221-2	1
NASA Flight Research Center	
P. O. Box 273	
Edwards, California 93523	
Attention: Library	1
Jet Propulsion Laboratory	
4800 Oak Grove Drive	
Pasadena, California 91103	
Attention: Library, Mail 111-113	1
NASA Manned Spacecraft Center	
2101 Webster Seabrook Road	
Houston, Texas 77058	
Attention: Library, Code BM6	1
NASA Marshall Space Flight Center	
Huntsville, Alabama 35812	
Attention: Library	1
NASA Wallops Station	
Wallops Island, Virginia 23337	
Attention: Library	1
NASA Electronics Research Center	
575 Technology Square	
Cambridge, Massachusetts 02139	
Attention: Library	1

# DISTRIBUTION LIST (Cont'd)

	<u>Copies</u>
NASA Lewis Research Center 21000 Brookpark Road Cleveland, Ohio 44135 Attention: Library, Mail Stop 60-3	1
NASA Goddard Space Flight Center Greenbelt, Maryland 20771 Attention: Library	1
NASA John F. Kennedy Space Center Kennedy Space Center, Florida 32899 Attention: Library, Code IS-CAS-42B	1
National Aeronautics and Space Administration Washington, D. C. 20546 Attention: Library, Code USS-10	1
John B. Parkinson, Code RAA	1
NASA Code RA	1
NASA Scientific and Technical Information Facility P. O. Box 33 College Park, Maryland 20740	14 plus reproducible



